Organic Electro-Optics and Optical Rectification: From Mesoscale to Nanoscale Hybrid Devices and Chip-scale Integration of Electronics and Photonics

Delwin L. Elder and Larry R. Dalton*
Department of Chemistry
University of Washington
Seattle, Washington 98195-1700

Delwin L. Elder
Department of Chemistry
Box 35170, Bagley Hall
University of Washington
Seattle, WA, USA 98195-1700
e-mail: elderdl@uw.edu
https://orcid.org/ 0000-0001-9302-3858

Larry R. Dalton
Department of Chemistry
Box 35170, Bagley Hall
University of Washington
Seattle, WA, USA 98195-1700
e-mail: dalton@chem.washington.edu
https://orcid.org/ 0000-0002-6461-0145

ABSTRACT

The performance of electro-optic devices based on organic 2nd order NLO materials has been improved by orders of magnitude through theory-guided improvement in the electro-optic activity and other relevant properties of organic materials and by field compression of radiofrequency (rf) and optical fields associated with the transition from microscale/mesoscale devices to silicon-organic hybrid (SOH) and plasmonic-organic hybrid (POH) devices with nanoscopic dimensions. This paradigm shift in organic electro-optic R&D has led to many performance improvements, including record performance for voltage-length performance of < 50 volt-micrometers (V-μm), energy consumption of < 70 attojoules/bit, bandwidths of > 500 gigahertz (GHz), and device footprints of < 20 μm^2. Another consequence of improving electro-optic performance is the corresponding improvement of the inverse 2nd order nonlinear optical property of optical rectification (transparent photodetection). Theory has permitted identification of optimum optical nonlinearity/transparency ratios and dipole moments for newly developed chromophores, which have led, in turn, to state-of-the-art materials and device performance.

1. INTRODUCTION.

In 1999, we provided an invited review of the development of organic electro-optic (OEO) materials and of waveguide devices based on such materials.[1] At that point in time, electro-optic waveguide devices, based on Pockels effect[2,3] materials such as lithium niobate and OEO materials, were quite large with waveguide lengths ranging from 1 to 10 centimeters (cm), electrode separations of 5 to 10 micrometers (μm), and waveguide widths of approximately 5 μm. Mathematically, the Pockels effect is given by $n_e(V) = n_e - (1/2)r_{33}n_e^3V$ where $n_e(V)$ is the extraordinary index of refraction of the material in the direction of an applied voltage (V); r_{33} is the relevant electro-optic (EO) coefficient of the material (the EO tensor element in the direction of the applied voltage); and n_e is the extraordinary index of refraction in the absence of an applied voltage.[3] The performance of electro-optic waveguide devices has been characterized by the voltage-length ($V_\pi L$—also referred to as $U_\pi L$) figure-of-merit, where V_π is the applied voltage required to produce a phase shift of π in a propagating optical wave and L is the electrode length (the distance over which the optical and electric (e.g., millimeter wave, microwave or radiofrequency) fields interact in the electro-optic material).

The simplest mathematical expression for $V_\pi L$ is $V_\pi L = (\lambda_o/2)(w/\Gamma)(1/(n_e^3 r_{33}))$ where λ_o is the optical wavelength, w is the electrode separation, and Γ is the overlap factor for the electric and optical fields in the OEO material.[3] This expression is for a push-pull waveguide Mach Zehnder modulator; the expression for a phase modulator is a factor of 2 larger.[3] In 1999, $V_\pi L$ values typically ranged from 2 to 20 V-cm.[1,4] Thus, while in our 1999 review, we demonstrated that electro-optic devices based on OEO materials could be integrated with wafer-scale, complementary-metal-oxide-semiconductor (CMOS) electronics,[1] integration of more than a modest number of devices was impossible because of the large $V_\pi L$. This mismatch between the sizes of electronic and photonic devices has been a major problem for the utilization of photonic devices for the chip-scale integration of electronics and photonics relevant to computing, telecommunications, sensing, and metrology. Also, in 1999, the resistance (RC-defined time response, which depends on electrode length) of metal electrodes limited bandwidth performance to approximately 100 gigahertz (GHz), although the fast (femtosecond) phase response of OEO materials could support much greater bandwidths (> 30 terahertz (THz)).[3] Around this period-of-time, Michael Hayden and others demonstrated THz spectroscopy and imaging techniques based on the utilization of thick film OEO materials.[5-11]

Second order nonlinear optic ($\chi^{(2)}$) materials facilitate not only translation of electronic information onto photonic (e.g., fiber and wireless) transmission (i.e., electro-optic (EO) modulation) but also of the reverse, i.e., conversion of photonic information carried on an optical carrier into electrical current (optical rectification (OR)). In 1999, optical rectification in the gigahertz frequency range (for waveguide-based telecommunication and sensor applications) was essentially unknown in Pockels type devices and so did not merit review. That situation has changed dramatically over the following 22 years as will be discussed in this review. It is important to note that optical rectification based on thick film devices for terahertz generation existed previously[5-11] and has been used for a variety of applications ranging from spectroscopy to imaging. The responsivity of optical rectification increases with frequency so that applications in the GHz range are more challenging than for the THz range.

The electro-optic activity (r_{33}) of lithium niobate is approximately 30 pm/V [i.e., An optical phase shift of 30 picometers occurs with application of an applied voltage of 1 volt]. In 1999, the r_{33} values of OEO materials were comparable.[1,4] The major argument at that time for using OEO materials was the femtosecond phase relaxation time of the conjugated π-electron systems of such materials. However, this fast response time of OEO materials to applied time-varying electric fields was not the device bandwidth defining factor; that was the resistivity of metal electrodes as already noted. While efforts to commercialize single waveguide devices based on OEO materials appeared in the early 2000s (Pacific Wave Industries and Lumera (now GigOptix), among others), the advantage of such materials was not sufficiently compelling to effectively compete with existing technologies based on Pockels effect lithium niobate or alternative approaches based on electro-absorptive materials or modulated lasers.[3,12] Materials such as lithium niobate have important advantages such as very low optical propagation loss and high thermal stability. Materials such as electro-absorptive materials afford advantages such as small device footprints and high bandwidth but at the expense of higher optical loss. No single material satisfies all electro-optic (EO) application requirements.

A sea change in electro-optic technology (and ultimately, optical rectification technology) has occurred with (1) the advent of the sub-wavelength technologies of silicon photonics and plasmonics[3,13-93] and with (2) theory-guided improvement of the r_{33} values and other relevant properties of OEO materials[89,92,93]. Silicon photonics and plasmonics have facilitated a dramatic reduction in device dimensions. Plasmonic-organic hybrid (POH) device lengths can be reduced to < 10 μm and electrode spacings to < 50 nanometers (nm). As illustrated in Figure 1, these dimensions permit a dramatic enhancement in electromagnetic fields (both rf and optical) in waveguides, leading to orders of magnitude reduction in $V_\pi L$ (approximately a factor of 100 for current POH waveguide devices and a factor of 1000 when improvements in r_{33} are considered). Indeed, $V_\pi L$ values of 40 to 50 V-micrometer have been reported for state-of-the-art (SOA) plasmonic-organic hybrid devices (see Figure 2--circles)[57,89,90] and even lower values will almost certainly be reported shortly based on demonstrated improvements in OEO materials (see Figure 2 novel materials--triangles).[89] The chemical structures of the chromophores of Figure 2 are given in Figure 3. $V_\pi L$ values of < 5 V-μm may be realized based on the use of smaller electrode spacings and further improvement of OEO materials. This would be a factor of 10,000 improvement in $V_\pi L$ since 2000. Optical insertion loss (the sum coupling loss, propagation loss and material absorption loss) is an important consideration for electro-optic device utilization. The loss associate with plasmonics and silicon photonics, as well as that of OEO materials, is of

concern. Key to the success of these nanophotonic devices is the utilization of short devices which minimize propagation loss. This, in turn, requires active materials with large second order electro-optic activity and enhancement through field compression. Coupling loss must also be considered and will, of course, depend on device architecture. Thermal and photochemical stability are also important for device applications. Thus, focus on a single performance parameter is not adequate for guiding improvement of device performance.

Of course, the transition from microscopic to nanoscopic electrode separations has been accompanied by recognition of new phenomenon including the attenuation of electric-field-poling-induced electro-optic activity with decreasing electrode separation. This attenuation is associated with interaction between chromophore dipoles and conduction electrons of the metal electrodes.[55,57,64,89,90] Another important consequence of small plasmonic-organic hybrid (POH) electrode separations is the increasing importance of the "slow light" effect for enhancing electro-optic activity (see Figure 4).[46,49] The slow light effect is associated with the slower propagation of surface plasmon polaritons (SPPs) relative to photons. The slower propagation results in a longer integration time for the electro-optic (EO) interaction and thus enhancement of the effect. The low RC values of plasmonic devices permit THz bandwidths to be realized (note that plasmonics involves converting photons into propagating plasmon polaritons with properties intermediate between photons and electrons). Indeed, in telecommunication applications, operational bandwidths of > 500 GHz have been reported[66,68,71]; and in sensor applications, bandwidths of greater than 1 THz have been demonstrated[73,75]. Device bandwidths of > 30 THz are theoretically possible.[3] Utilization of nanophotonic devices has also permitted a dramatic improvement in energy efficiency of electro-optic devices; values of < 70 attojoules/bit (for digital information processing) have been achieved in strip-line (single pass) devices[67] and much smaller values are possible with resonant (e.g., ring resonators) devices due to resonant enhancement associated with the quality (Q) factor of such devices. Utilizing the latest improved OEO materials will likely lead to energy efficiencies of < 10 attojoules/bit even for strip-line devices. The combination of the introduction of nanophotonic device technologies together with improvements in OEO materials has permitted the practical integration of electronics and photonics.[74,89] Another important achievement has been the integration of OEO materials into free space metasurface devices, which represents a significant advance in sensor and display technology.[82-84]

Optical rectification at GHz frequencies (relevant to telecommunications, computing, and sensing) was first observed in a silicon-organic hybrid (SOH) waveguide device in 2005.[21] Michael Hayden and others had previously pioneered the use of optical rectification at THz frequencies.[5-11] The absence (or reduced presence) of phonon modes in OEO materials in the frequency range 1-15 GHz makes these materials attractive for applications such as spectroscopy and imaging. In 2005, the responsivity (R) at GHz frequencies was still well below of the value of commercial inorganic photodiode devices (approximately 1 Ampere/Watt) and so the 2005 observation was not further pursued at that time. However, two interesting features were observed in this initial study, namely, very high bandwidth performance and a very low noise floor. Note that unlike conventional photodiodes (traveling wave uni-traveling carrier photodiodes, TW-UTC-PD; p-i-n traveling wave photodiodes, p-i-n TW-PD; ultra-broadband-carrier photodiodes, UBC-PD), optical rectification does not involve electron excitation and thus can be viewed in the low material absorption limit as "transparent photodetection". Through the 2nd order NLO effect of OR, the optical field produces a potential between the electrodes causing current to flow. Unlike conventional photodiodes, the responsivity of OR increases (in an approximately linear manner) with increasing frequency, rather than being flat with increasing frequency and falling precipitously at some high (GHz) frequency (due to the excited state lifetime of the photoexcited electrons) as is the case with inorganic photodiodes. The simplest mathematical expression for optical rectification responsivity (R) is $R = (i/P) = |(n_e^3 r_{33}/2c)f(w/\Gamma')(L/A)|$ where i is the OR-induced current in Amperes, P is the optical power in Watts, n_e is the extraordinary index of refraction, r_{33} is the principal element of the electro-optic tensor, c is the speed of light, f is the modulation frequency on the optical carrier, w is the electrode separation, Γ' is the overlap of the optical field with the 2nd order nonlinear optical material, and A is the waveguide cross-section area. This expression reasonably accounts for the responsivity of Pockels effect materials for mesoscopic devices. The expression is more complicated for nanophotonic plasmonic devices (which is also the case for electro-optic modulation—see Figure 4). Both EO and OR depend on $n_e^3 r_{33}$. Following the 2005 publication, Baehr-Jones and coworkers[91] estimated that responsivity values of 9 mA/W at 400 GHz could be achieved with OEO materials exhibiting an in-SOH-device EO activity of 300 pm/V. With improved electric field concentrations associated with the use of a 50 nm electrode separation in POH devices and r_{33} values of 1000 pm/V, responsivity values can be improved to 1.8 A/W,[89] which is competitive with the best inorganic photodiode devices but affording much

superior bandwidth performance and a lower noise floor (to be discussed later in relation to spur free dynamic range and bit error rate). Even smaller electrode spacings are desirable. However, it is important to note that research involving OR is in a very immature state: indeed, the mechanisms defining noise floor for Pockels materials remain to be defined experimentally. Cox and coworkers recently published one of the first detailed studies (utilizing lithium niobate).[94]

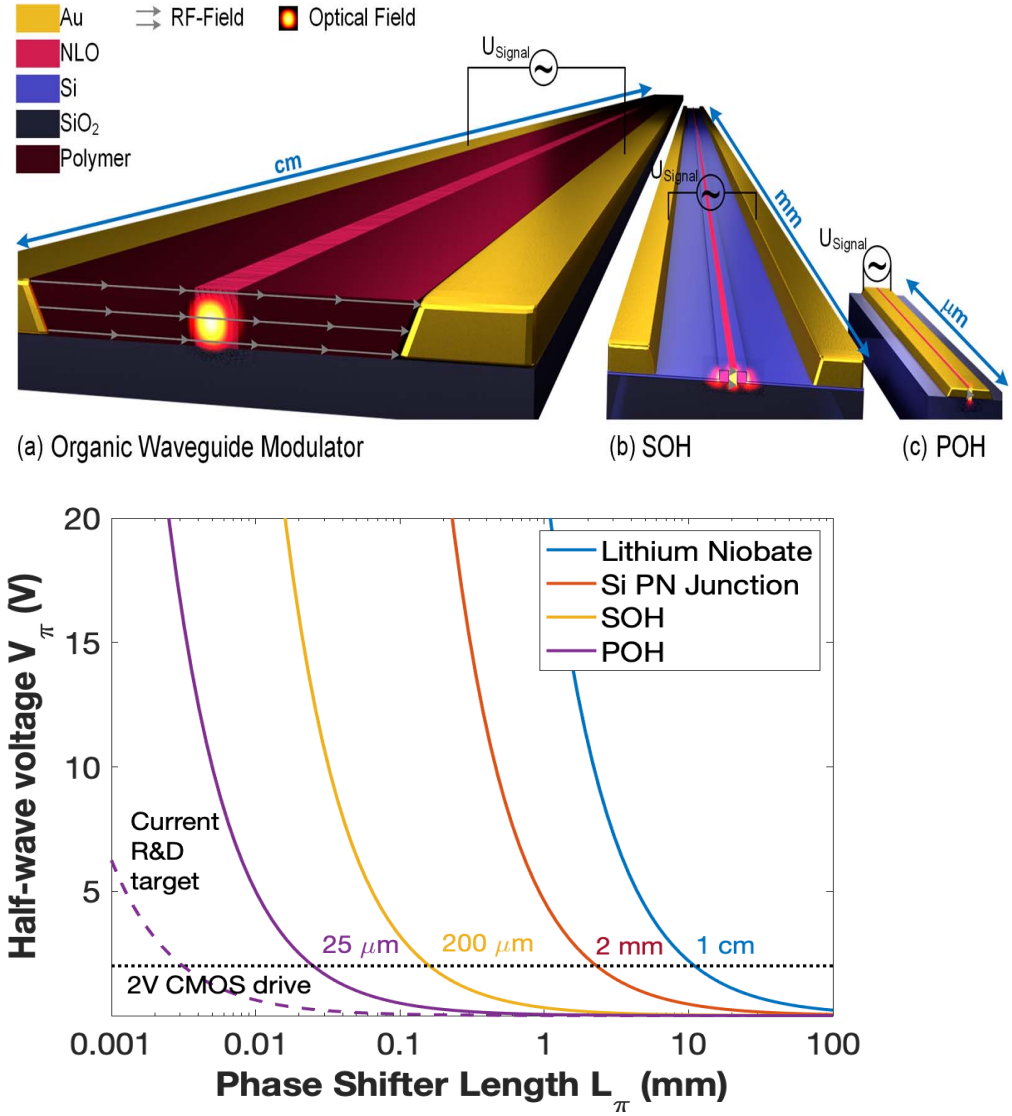

Figure 1. Upper: Variation of device size for various types of modulators is schematically illustrated. SOH stands for silicon-organic-hybrid device; POH stands for plasmonic-organic-hybrid device. Note that $U_\pi L$ and $V_\pi L$ will be used interchangeably as both appear in the literature. Adapted from reference 52 with permission. Lower: The variation of halfwave voltage (V_π) with electrode length/device length (L) is shown for various types of devices and for the POH research goal. Adapted with permission from reference 89.

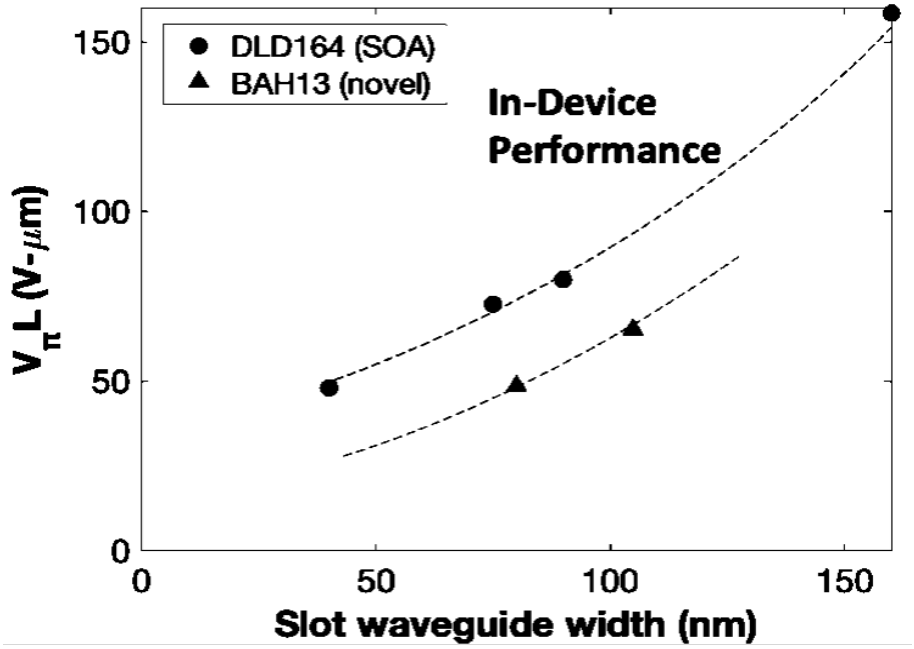

Figure 2. Variation of $V_\pi L$ with waveguide slot width (electrode separation) is shown for a state-of-the-art chromophore DLD164 and preliminary data are shown for a newly prepared (novel) chromophore BAH13.[90,93] In the absence of chromophore-electrode electrostatic interactions, $V_\pi L$ would be predicted to decrease in a linear manner with decreasing w. Even without addressing the attenuation problem, the use of smaller waveguide widths should lead to voltage-length values < 40 V-μm using BAH13. The chemical structures of DLD164 and BAH13 are given in Figure 3. Adapted from reference 90 with permission.

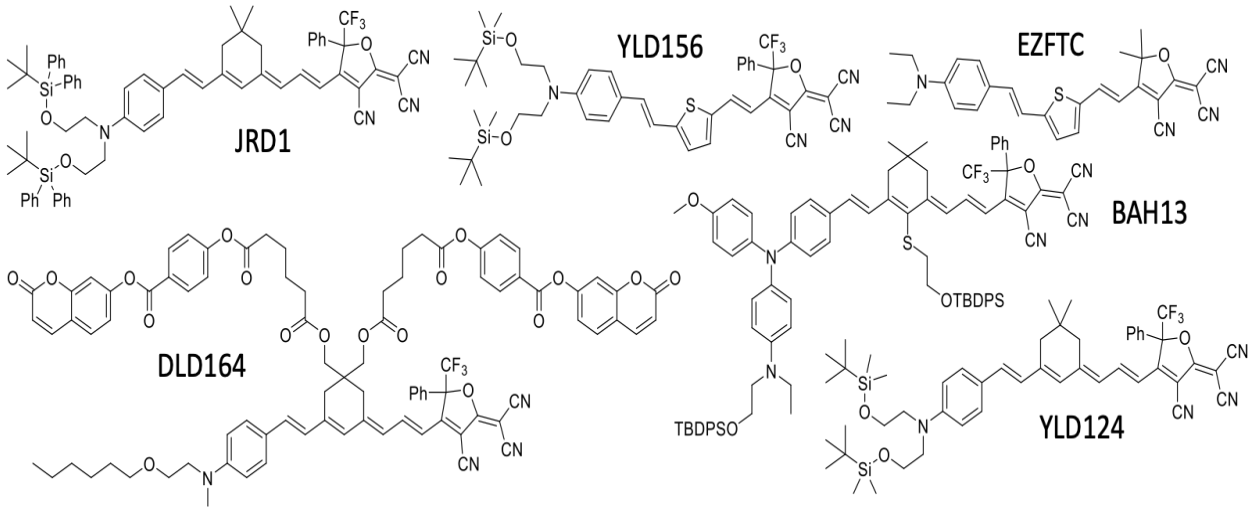

Figure 3. Early chromophores (JRD1, EZFTC, YLD124, YLD156 and DLD164) are shown together with the recently synthesized chromophore BAH13.

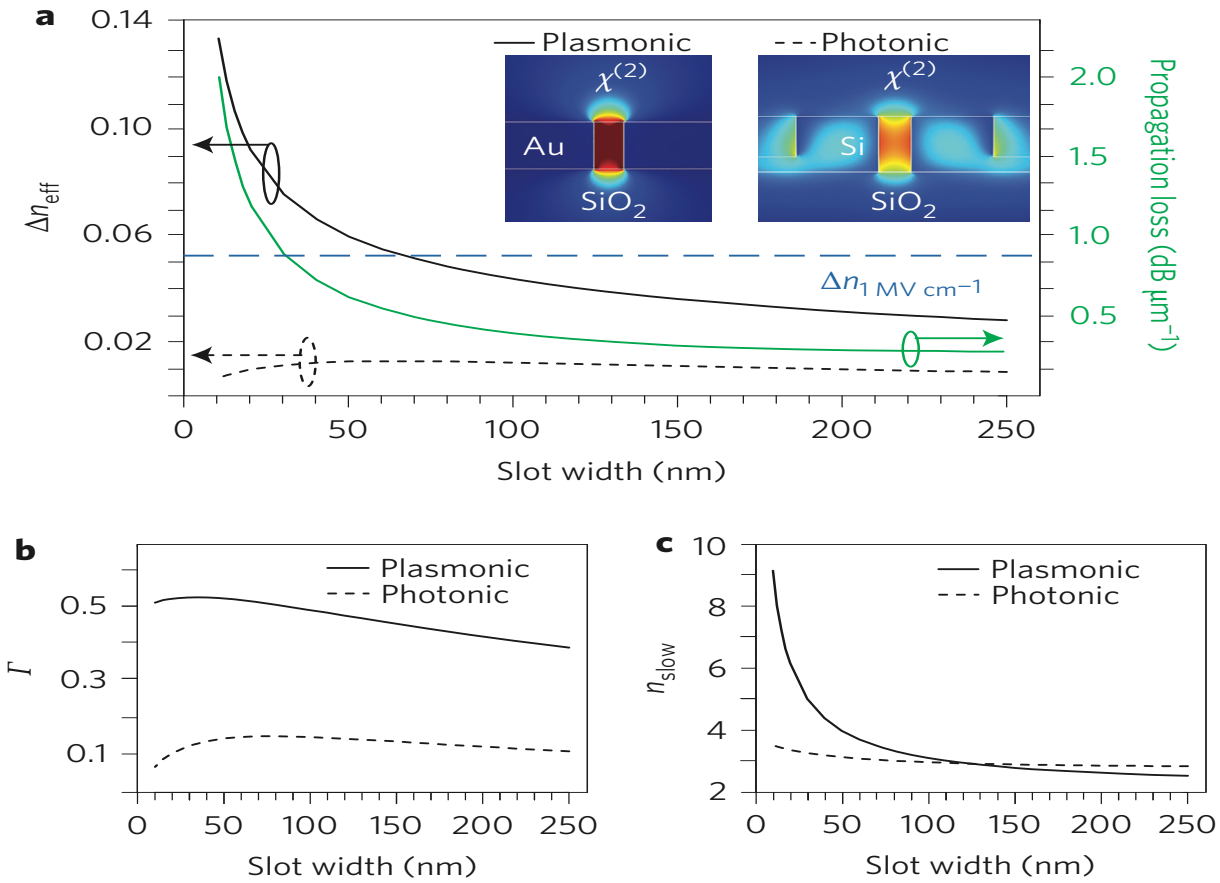

Figure 4. (a) $\Delta n_{eff} = \Gamma(\Delta n_{mat}/n_{mat})n_{slow}$ where Δn_{eff} is the index of refraction change induced in a plasmonic waveguide, containing an OEO material, by an applied electric field, Γ is the field energy interaction factor for the optical field confined to the slot and polarized parallel to the active axis of the OEO material, Δn_{mat} is the index of refraction change induced in the OEO material by the applied electric field, and n_{mat} is the index of refraction of the material in the absence of the applied electric field. The solid line is for a plasmonic slot waveguide, and the dashed line is for the equivalent photonic silicon waveguide. The electric field in both slots is 1 MW/cm. Also shown is the propagation loss as a function of slot width. (b) The variation of Γ is shown as a function of slot width for plasmonic and photonic waveguides. Much tighter field confinement is observed for plasmonic devices. (c) The dependence of the slow light effect (n_{slow}) is shown as a function of slot width for plasmonic and photonic waveguides. Adapted with permission from reference 46.

Another important consequence of moving from microscopic electrode separations, w, to nanoscopic widths is the opportunity to transition from processing protocols based on electric field poling[3] to protocols based on use of covalent bonds (sequential-synthesis/self-assembly)[3,95-99] for the introduction of acentric order. The large values of electrode separations (w) of mesoscopic devices in the year 1999 made sequential-synthesis/self-assembly impractical because of the excessively large number of sequential steps required. This approach becomes feasible with w values < 50 nm. It is also important for addressing interfacial interactions between gold electrodes and electrically-poled OEO materials that lead to reduction in desired acentric order. Sequential-synthesis/self-assembly also can lead to improved thermal and photochemical stability.[3]

This review focuses on an introduction to and review of the details of multi-scale (quantum/statistical mechanical) theory-guided improvement of 2nd order NLO materials and upon the utilization of nanophotonic (subwavelength) silicon photonic/plasmonic devices. Its focus is on chromophores to devices R&D rather than just on materials. It is not a comprehensive review of the literature associated with electro-optics. For example, numerous articles have appeared focused on using conventional DFT functionals and traditional wavefunction methods to calculate molecular first hyperpolarizabilities. For the most part, these

articles do not involve comparison of theory with experiment, nor do they lead to the synthesis of new state-of-the-art materials and their integration into devices. While such articles provide very useful insights, they do not typically provide important "molecules to devices" guidance for optimizing electro-optic technology that is the focus of this review and thus will not be reviewed here. Optical nonlinearity, optical transparency (optical absorption), and dipole moment are important parameters for identifying the best chromophores and theoretical guidance permits identifying chromophores yielding the optimum value of these properties. Specifically, theory permits definition of optical nonlinearity/optical transparency products (or optical nonlinearity/optical absorption loss ratios) for chromophores, which is critical for the selection of appropriate chromophores for specific devices, e.g., plasmonic-organic hybrid and silicon-organic hybrid devices. Theoretical predictions can be calibrated by comparison with experimental determinations of molecular first hyperpolarizability measured by hyper Rayleigh scattering (HRS) and absorption measured directly and by variable angle spectroscopic ellipsometry (VASE).[93] Avoiding chromophores with excessively large dipole moments is critical if acceptable levels of acentric order are to be achieved by electric field poling or sequential-synthesis/self-assembly processing protocols. Such information is central to the systematic improvement of the performance of OEO materials.

In like manner, some aspects of device architecture optimization will not be reviewed, e.g., linearization of the modulator response function for improvement of signal linearity (spur free dynamic range (SFDR)[57,86,100-102] and bit error rate (BER)[46,49,52,54,57,61,64,65,67-69,72,76,78]). While this is an on-going area of research involving device architectures, it is largely independent of material used and is defined by device/system architecture. We will, however, provide examples of typical SFDR and bit-error-rate (BER)[78] performance for hybrid organic EO devices. In like manner, we will not do a detailed comparison of modulator technologies (modulated lasers, Pockels effect modulators, and modulator based on electro-absorption and other mechanisms) as these are covered in many cited reviews.[3,12,17-20,51,52,57,101-104] We do note that new classes of EO materials (e.g., such as ITO[103]) are emerging and merit attention. Our perspective is to provide insight into coordinated development of OEO materials and related devices relevant to commercial (or potentially commercial) electro-optic and optical rectification technologies. The current review also attempts to avoid repeating material covered in other reviews.

This review emphasizes the need to change research perspectives with respect to OEO materials based on emerging data and the importance of simultaneously considering both materials and device architectures in implementing new technologies. The paradigm shift in R&D since 1999 has already led to orders of magnitude improvement in $V_{\pi}L$, device footprint, energy efficiency, bandwidth, signal quality (spur free dynamic range, SFDR, for analog signal processing and bit error rate, BER, for digital signal processing). Chip-scale integration of electronics and photonics not only affords dramatic improvement in performance but also permits important cost reduction and improvement in reliability. In engineering parlance, this means improvement of size, weight, power, cost, and performance (SWaP-CP).

The following sections focus on (1) theory-guided development of new OEO materials and on (2) the role of device architecture on device and system performance. These sections are followed by a consideration of auxiliary properties of thermal and photochemical stability and of issues related to characterization and chromophore synthesis. The final section focuses on what can be expected for the future development of integrated electronic/photonic technologies and on applications of the technology. The application space is amazingly broad ranging from computing, signal processing, metrology, and telecommunication to a plethora of sensor applications such as Lidar[105-107], Radar[108], optical gyroscopes[109], embedded network sensing, the Internet of Things (IoT), and including sensing of both chemical and physical phenomena.

A comment on the changing R&D perspective with respect to OEO materials since the late 1980s and early 1990s is appropriate. In the latter quarter of the last century, a significant number of major corporations and academic researchers pursued organic electro-optic materials research by initially dissolving commercially available chromophores (such as disperse red chromophores[3]) in commercially available polymers (e.g., PMMA, PC, PI, etc.[3]) and electrically poling the resulting composite materials near their glass transition temperatures. The research of this period is easily accessed in SPIE and MRS conference proceedings of the time. The modest molecular first hyperpolarizabilties of early chromophores, the modest poling efficiencies of early composites, and the poor thermal and photochemical stabilities of early materials (defined by the low glass transitions of the composites) inhibited the effective commercialization of these early materials and R&D in this area was largely abandoned by early practitioners. In the late 1990s, the issue was whether-or-not the performance of OEO materials could be improved in a timely manner by developing chromophores with improved molecular first hyperpolarizability,

materials with improved poling efficiencies, and hardened materials yielding improved stability, Clearly, numerous structure/function relationships had to be defined in a finite space of time. To accomplish this in a timely manner required guidance from theory together with collection of a daunting array of experimental data. Given the state of theoretical methods at the time, improved computational methods had to be developed and calibrated against experimental measurements. Previously ignored problems such as the impact of intermolecular electrostatic interactions among chromophores needed to be explicitly addressed and this required development of new computationally efficient, coarse-grained statistical mechanical methods. Both quantum and statistical mechanical methods capable of evaluating a wide range of material options in a short space of time were required. In like manner, new and improved experimental methods were required. Measurements of absolute values of molecular first hyperpolarizabilities, acentric order, and electro-optic activity in bulk materials range from challenging to unrealistically difficult. The ultimate interest is the electro-optic activity and optical loss of materials in devices, which can be determined with high accuracy. Intermediate steps, in the evolution from chromophores to devices and systems, must identify improved chromophore structures and material processing protocols. In this down selection process from many options, the relative performance of chromophores and materials is more relevant than absolute values for a particular chromophore or material. Thus, while measurement of absolute values of molecular first hyperpolarizabilities of chromophores by hyper Rayleigh scattering (HRS) is unrealistically difficult, it is relative values that are relevant to the optimization of OEO for device applications. Various methods of determining bulk electro-optic activities, such as Teng-Man[3] and ATR[3], represent different levels of difficulty and accuracy. ATR permits determination of r_{33} and r_{13} and avoids some of the complications associated with the Teng-Man method; however, it is not appropriate for screening of large numbers of materials. The smaller number of ATR measurements that can be executed in a finite amount of time are reserved for verifying more easily executed Teng-Man measurements and for characterizing acentric order parameters through the theoretically defined relationship to the ratio r_{33}/r_{13}. Teng-Man permits *in situ* measurement of poling-induced EO activity and is thus useful in characterizing the relative poling efficiency of different poling protocols including the details of multi-layer device architectures used to control material conductance relevant to poling efficiency and device operation. These detailed studies provide important insights into the dependence of performance on poling architectures and are useful in identifying measurement artifacts such as the effect of multiple reflections in multilayer poling architectures. Selection criteria for optimized chromophores and materials depend on multiple parameters including molecular first hyperpolarizability, absorption loss, dipole moment, chromophore shape (intermolecular electrostatic interactions), electro-optic activity, index of refraction, and dielectric permittivity. Correlation of a large amount of theoretical and experimental data is required, together with practical insights into chromophore synthesis and material processing realities. Above all, improvements must be accomplished is a timely and resource utilization efficient manner, which necessitates hard decisions with respect to the allocation of resources. Finally, transition of R&D to nanophotonic devise brings a new level of complexity with performance depending on the details of interfacial interactions. Nanophotonic devices require new test (characterization) protocols as will be discussed later in this review. The new nanophotonic testbed (shown in Figure 22) affords the characterization of electro-optic activity in-device-relevant structures, permits systematic investigation of the influence of device architecture on achievable in-device material EO activity, and permit more accurate measurement of electro-optic coefficients. Clearly, the complexity of OEO material and device R&D has increased dramatically over the past two decades but the utility of the protocols discussed is evident in the improved performance of POH and SOH devices. Hopefully, this review provides insight into a systematic approach to addressing the complexity of optimizing OEO materials and devices in a timely manner.

2. **Theory-Guided Improvement in OEO Materials**.

For introductory material related to nonlinear optics and theoretical/experimental methods, the reader is referred elsewhere.[3,110-168] An overview of the workflow for multiscale theory-guided improvement of 2nd order NLO materials is illustrated in the accompanying Figure 5.

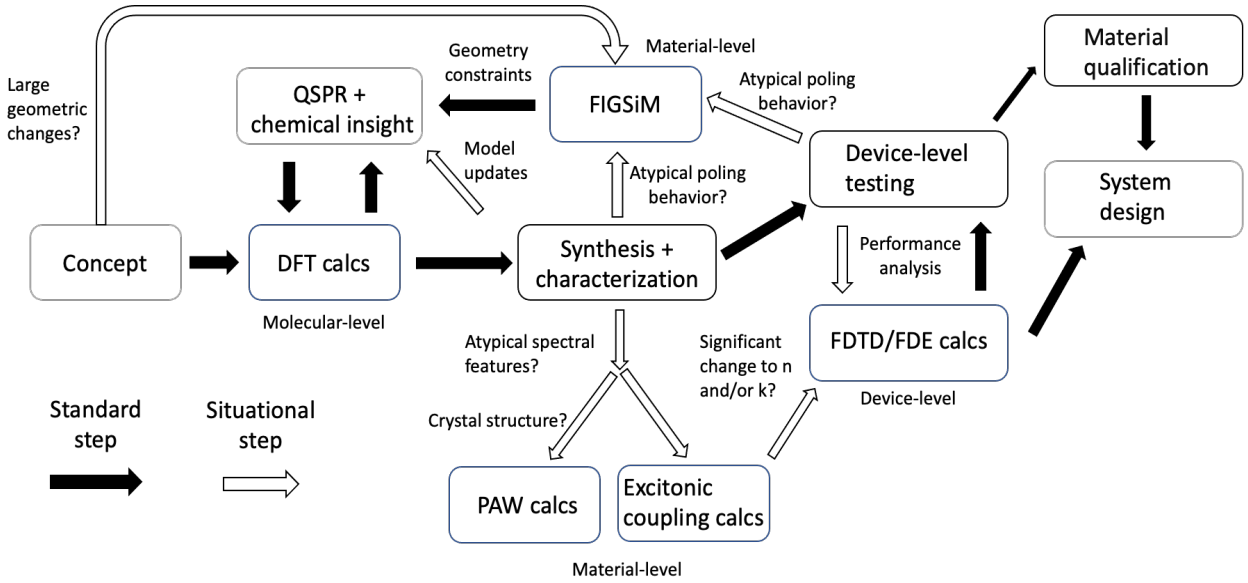

Figure 5. The workflow for multiscale improvement and evaluation of 2nd order NLO materials and their accompanying devices is shown. QSPR = quantitative structure-property relationship, DFT= density-functional theory (Gaussian commercial), PAW = projector-augmented wave (VASP, commercial), FIGSiM = finite improbability generator for simulation of materials (in-house, open source), Excitonic coupling = collaboration with Isborn group[126,127] (homebrewed code) for intermolecular effects on optical and nonlinear optical properties, FDTD/FDE = electrodynamics simulations (Lumerical, commercial). This Figure was prepared by Dr. Lewis Johnson.

In the following sections, it will become clear why it is important to employ an end-to-end, multiscale consideration to optimize system performance. Initial quantum mechanical calculations involved use of early wavefunction and density functional theory (DFT)/time-dependent density functional theory (TD-DFT) methods to evaluate molecular first hyperpolarizability for molecules *in vacuo* and in the long wavelength (zero frequency) limit. Improved calculations required addressing the effect of dielectric environment (including chromophore aggregation) and of frequency (including resonance effects) and benchmarking against higher order computational methods.

At the material level, electro-optic activity requires introduction of acentric order. This has most commonly been accomplished by electric field poling of neat chromophore materials or chromophore-containing polymers/composites near their glass transition temperature. Strong chromophore-chromophore dipolar interactions oppose poling-induced order. Indeed, chromophores with the highest dipole moments are unusable. Detailed intermolecular electrostatic interactions must be explicitly considered to understand poling-induced order. Such considerations have led to site-isolation through steric modification of chromophores, to the introduction of multi-chromophore dendrimers and binary chromophore glasses, to introduction of electrostatic moieties that influence matrix dimensionality (i.e., reducing matrix dimensions from 3-D to 2-D or even to 1-D noting that fractional dimensionalities are also possible) and to other matrix-assisted poling phenomenon. Theoretical considerations have also led to new processing protocols such as laser-assisted electric field poling (LAEFP)[110] (which is an example of matrix-assisted poling) and to new material characterization techniques such as variable angle polarization-referenced absorption spectroscopy (VAPRAS)[111]. For the sake of simplicity, we separate the review of quantum and statistical mechanical methods although in practice these are considered together. Also considered simultaneously with theoretical insights are consideration of device architectures (including interfacial interactions) and material synthesis and processing issues.

2.1. Improvement of Molecular Properties: Molecular First Hyperpolarizability and Linear Optical Properties. The relationship of the components of electro-optic activity (r_{33}): [molecular first hyperpolarizability β, chromophore number density ρ_N (also referred to as N), acentric order $\langle\cos^3\theta\rangle$ where

θ is the angle between the applied electric fields and the principal axis of the hyperpolarizability tensor, and dielectric(ε)-index of refraction(n_e)] is shown in Figure 6 (right side).

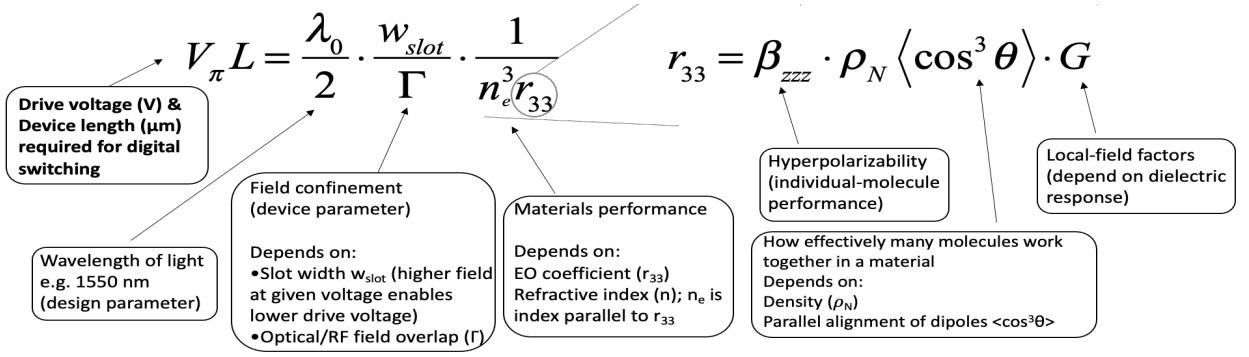

Figure 6. Simple expressions for $V_\pi L$ and r_{33} are shown as a function of component terms.[89] Note that both β_{zzz} and $\langle\cos^3\theta\rangle$ are dependent on ρ_N. Figure modified from reference 89 with Permission.

In 1999, theoretical guidance for the improvement of molecular first hyperpolarizability involved use of early density functional theory (DFT) together with traditional wavefunction based methods.[1,3,112-125] Since that time, use of improved DFT functionals, treatment of dielectric and frequency efforts, and treatment of chromophore aggregation effects have led to greatly improved prediction of linear and nonlinear optical properties.[64,89,90,92,93,126-139] A example of the importance of dielectric effects is shown in Figure 7.

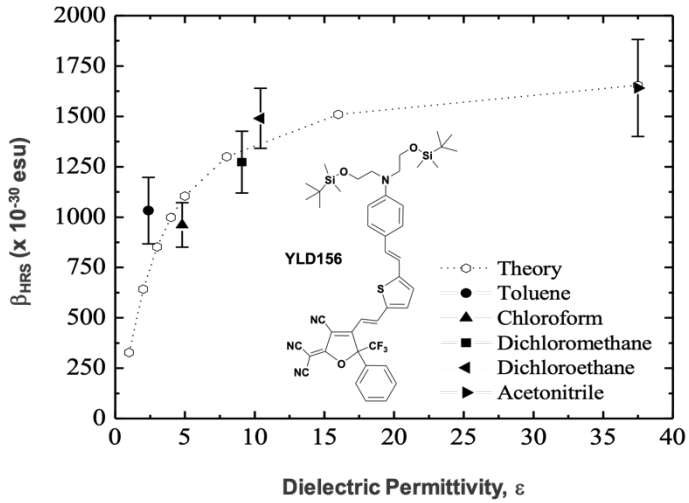

Figure 7. The theoretical (DFT) and experimental variation of molecular first hyperpolarizability with dielectric permittivity is shown.[124] Adapted from reference 124 with permission.

Indeed, large scale surveys (Figure 8 Left Side) of putative chromophore structures are now possible with good confidence (expected correlation of theoretical and experimental hyperpolarizabilities as shown in Figure 8 Right Side).[89] Structures of chromophores are given in Figures 3 and 9. Theory provides critical insight into optical nonlinearity/optical transparency products and dipole moments. For example, the optical nonlinearity(β)/absorption loss(k) ratio for BAH13 is significantly greater than that of BAY1 even though BAY1 is theoretically and experimentally observed to have the higher molecular first hyperpolarizability. The concept of an "optical nonlinearity/optical transparency trade-off" only applies rigorously to structure variations within a simple class of chromophores (e.g., short NGS chromophores). Theory also illustrates that the optimum dipole moment value is that for JRD1 (which also has a superior optical nonlinearity/optical absorption loss ratio). The importance of these theoretically predicted (and experimentally verified) chromophore properties is borne out by their leading to superior device performance for both POH and

SOH devices. BAH13 is currently the material of choice for POH device applications and JRD1 is currently the current material of choice for SOH device applications. Lower material loss is required for SOH devices because the optical loss of silicon waveguides is much less than plasmonic waveguides and the material loss requirement is that it be less than or equal to the loss of the passive waveguide materials.

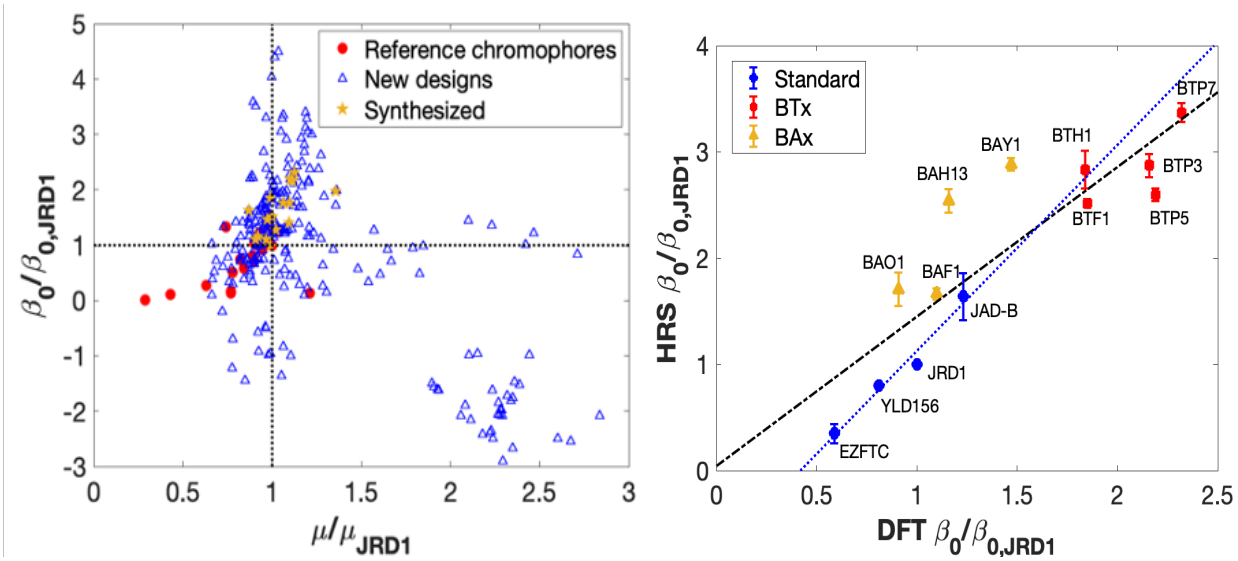

Figure 8. Left: Theoretical values of long-wavelength-limit molecular first hyperpolarizability (β_0), referenced to those of the workhorse chromophore JRD1, are shown as a function of computed chromophore dipole moment (μ) also referenced to JRD1. Well-known (reference) chromophores are shown as red circles. Recently designed (new) chromophores are shown as blue triangles. Newly synthesized chromophores are shown as yellow triangles showing predicted improvement in β_0. Right: Theoretical β_0 values referenced to JRD1 are shown as a function of β_0 values determined by hyper-Rayleigh scattering (HRS) measurements (also referenced to JRD1). Blue circles indicate values for well-known (standard) chromophores. The theoretical trend predicted for these chromophores is in good agreement with HRS measurements. Yellow and red symbols are for newly considered chromophores. The agreement between theory and experiment is less good but still useful in predicting trends. The degraded agreement may be due to inadequate treatment of dielectric (reaction field) effects and of frequency effects using the two-state model. The value of β_0 for BAH13 is 2680 x 10^{-30} esu while the value for BAY1 is 3040 x 10^{-30} esu.[93] The most-commonly-utilized DFT method is M062X/6-31+G(d) in PCM. Structures for the chromophores of Figure 8 Right are given in Figures 3 and 9. Adapted from reference 89 with permission.

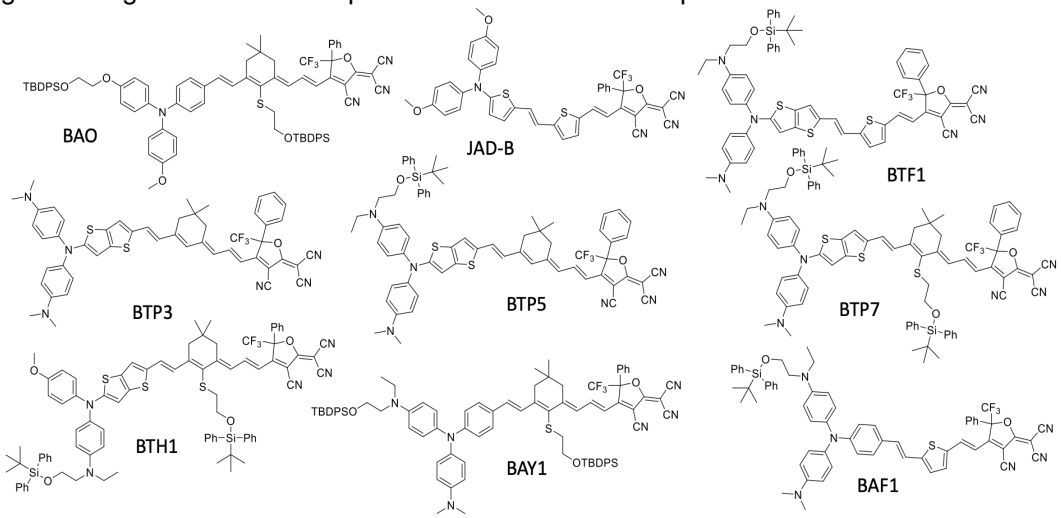

Figure 9. The chemical structures of some recently synthesized chromophores are shown. See Figure 8 for the theoretical and experimental β_0 values for these chromophores.

Most chromophores used in devices fall into the category of neutral ground state (NGS) chromophores that can be viewed within the context of a two-state model where the excited state is viewed as a zwitterionic (charge separated) state (ZES). Chromophores with large dipole moments (such as zwitterionic ground state, ZGS, chromophores—chromophores on the right side of Figure 8 Left) are to be avoided as strong dipole-dipole interactions oppose the introduction of desired acentric order (finite $<\cos^3\theta>$). The ground state of chromophores can, in general, be viewed as an admixture of the neutral and zwitterionic states with the exact nature of the admixture defined by donor and acceptor strengths and by the connecting π-electron bridge. As pointed out by Marder and coworkers[112-114], this leads to an impact on bond length alternation. The two-state model is often used in discussing the frequency dependence of β values (the relationship between β_ω and β_0). An analytical expression for the simple two-state model (that neglects the details of individual chromophore structure) was introduced and extensively discussed by Marder and coworkers.[112-114] Numerical quantum mechanical data provide quantitative insight into the importance of various elements of the two-state model (ground state dipole, excited state dipole, transition moment, and charge transfer bandgap). Indeed, some of the most promising recent chromophores have modest ground state dipoles but very large excited-state dipoles leading to large difference values and large molecular first hyperpolarizabilities. The important point is that current theoretical methods permit reliable prediction of molecular hyperpolarizability, optical absorption, and dipole moment including the effect of excitonic intermolecular interactions on these parameters (to be discussed shortly). This greatly accelerates the down selection of viable chromophore structures.

An exception to simple two-state type chromophores are twisted-bridge chromophores introduced by Marks and coworkers.[140-142] These chromophores have been evaluated by various theoretical methods.[140-143] However, the large dipole moments of twisted bridge chromophores have proven to be a serious impediment for their use in devices.

Quantum mechanical calculations of many-atom OEO chromophores have also provided important insights into index of refraction and dielectric properties.[90] Because index of refraction affects electro-optic activity through the expression $n_e^3 r_{33}$, the impact of n_e variation with chromophore structure and order can be large. Indeed, the effect of matrix dimensionality on r_{33} appears to be dominated by the impact of dimensionality on n_e.[90]

In recent years, considerable progress has been made in the development of quantum mechanical methods, particularly as related to analyzing the impact of chromophore-chromophore intermolecular excitonic interactions.[126,127] These results are relevant not only for understanding nonlinear optical properties but also for understanding the optical spectra of solid-state organic materials. Such calculations have relied on using both quantum mechanics and statistical mechanics and have proven crucial to understanding optical, nonlinear optical, dielectric, and index of refraction properties in a unified way. It is interesting to note that chromophore-chromophore π-electron interactions have a dramatic impact on linear optical spectra but very little effect of electric-field-poling-induced electro-optic activity for materials with low $<\cos^3\theta>$ values. Recently, the effect on optical spectra of solid-state materials has been effectively simulated as shown in Figure 10. The impact on r_{33} depends on the relative orientation of chromophores; and for low poling efficiency ($<\cos^3\theta>$ less than 0.2), chromophores are nearly randomly disordered. The enhancements and attenuations of EO values are averaged out for materials with low acentric order so the net effect is small.

The need for reliable quantum mechanical modeling is evident from a consideration of Figure 8. The possibilities for chromophore modification are simply too great to use an Edisonian approach for the development of improved chromophores. Down selection of putative structures based on theory is critical given limited time and synthetic resources. From a consideration of Figure 8, it is obvious that theory permits identification and avoidance of high dipole moment chromophores that cannot be processed into the desired non-zero acentric order materials. Theory also permits down selection of chromophores that have the desired optical and dielectric properties. Of course, synthetic feasibility must also be considered. Over time, the importance of correlating quantum and statistical mechanical methods has been realized as electro-optic devices require solid-state OEO materials containing finite chromophore concentrations. Development of such correlated multi-scale theoretical methods over the past decade has been critical to dramatically improving the performance of materials in devices. DFT methods, that have benchmarked against higher level (e.g., coupled cluster theory) methods, have guided order of magnitude improvement of molecular hyperpolarizabilities, have guided the identification of chromophores with acceptable optical loss, and have

guided the identification of chromophores with acceptable dipole moment values. The rate of improvement has slowed in recent years as the process has been optimized and even though further improvements in hyperpolarizabilities are possible, such improvements are likely to involve factors of 2 to 3 improvement rather than orders of magnitude improvement. The improved understanding of the impact of chromophore modification on index of refraction and dielectric properties will likely be more effectively exploited in the future.

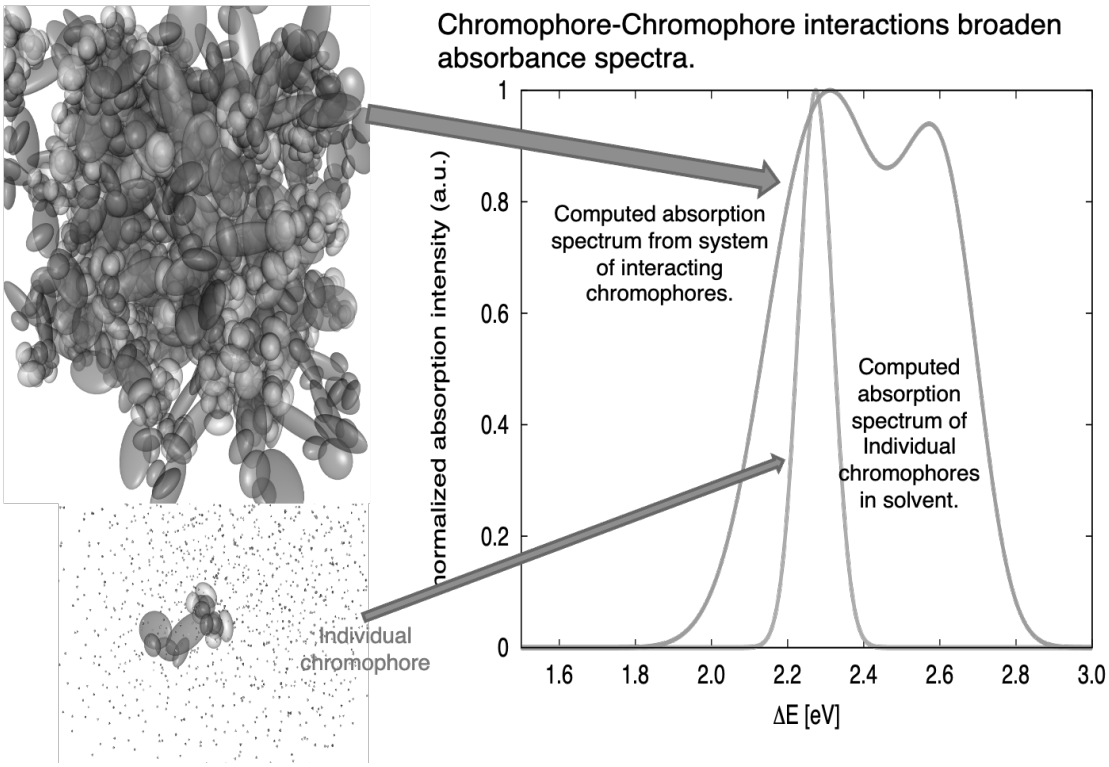

Figure 10. The simulated inter-band absorption spectra for "isolated or independent particle chromophores (in a uniform dielectric environment) and for interacting chromophores in solid state materials are shown for the YLD124 chromophore material. The simulation of the latter requires use of the chromophore distributions (ensemble order) identified by coarse-grained statistical mechanical calculations—discussed in the next section). Adapted from the collaboration with C. M. Isborn with permission from Prof. Isborn.[126,127]

Theory identifies the dipole moment of JRD1 as the optimum chromophore dipole moment for the introduction of acentric order. Optimum optical nonlinearity/optical absorption ratios will depend on device architecture. A selection criterion for chromophore absorption loss is that it does not exceed loss contributions from passive device elements. Thus, the optimum optical nonlinearity/absorption loss ratio for a POH device is represented by BAH13 while the optimum optical nonlinearity/absorption loss ratio for a SOH device is represented by JRD1 because the passive waveguide losses of silicon photonics are less than for plasmonic waveguide devices. Of course, chromophore structures must also be modified to achieve desired processing and realization of hardened materials. Without theoretical guidance, progress in improving chromophores would be unacceptably slow.

2.2. Improvement of Macroscopic (Molecular Assembly) Properties: Acentric Order and Chromophore Number Density. Understanding poling-induced order has required explicit treatment of both chromophore-applied field and chromophore-chromophore electrostatic interactions[1,3,144-168] and more recently of chromophore-electrode interactions (for nanoscopic devices)[55,57,89,90]. This has been accomplished by development of both analytical[1,3,147,152,153,156,157] and numerical simulation[3,148-151,157-168] analyses. Analytical methods involved approximation of chromophores as single prolate ellipsoids. The results indicated the importance of chromophore shape and of modifying chromophore cores to change shape (and thus chromophore-chromophore steric interactions). This information has been widely used to

improve poling induced order. A rigid body approximation to chromophore structure is appropriate in first order because the conjugated π-electrons restrict chromophore flexibility.

To achieve more accurate simulations of chromophore-containing materials, more detailed information with respect to chromophore structure is required. Fully atomistic simulations are too time demanding to evaluate a significant number of materials.[144-146] This problem has been addressed by Andreas Tillack and coworkers[161,165-168] through development of the level of detail (LoD) method (Figure11) and the adiabatic volume adjustment (AVA) acceleration method (Figure 12).[161,165-168] These methodological improvements have permitted reasonable (time-efficient) course-grained, accelerated simulations of material systems containing large numbers of complex chromophores. An important observation of these simulations is realization of the interconnection of chromophore number density, ρ_N; dipole moment, μ; and acentric order, $\langle\cos^3\theta\rangle$ (see Figure 13). This illustrates that, among other things, steric modification of the chromophore becomes counter-productive beyond a certain point with respect to increase in radius of chromophores because of its effect on decreasing ρ_N. Simulations also identified the potential for good performance with neat chromophore materials (chromophores with high number densities).

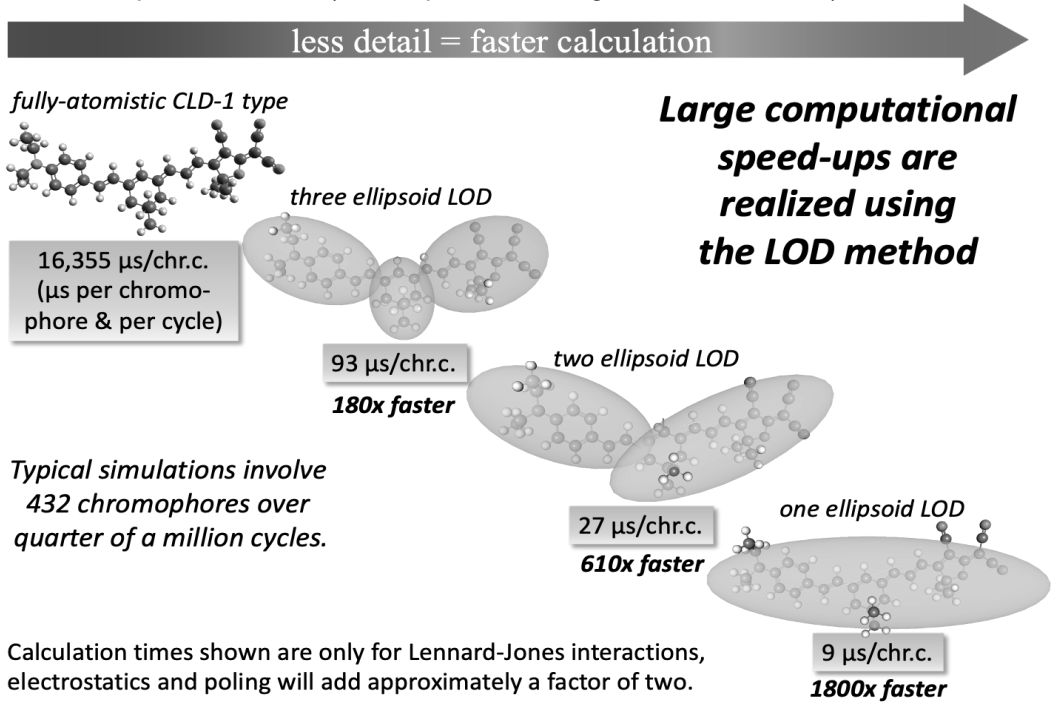

Figure 11. A trade-off between computational speed and level of detail in representing chromophores is illustrated. Figure generated by Dr. Andreas Tillack.

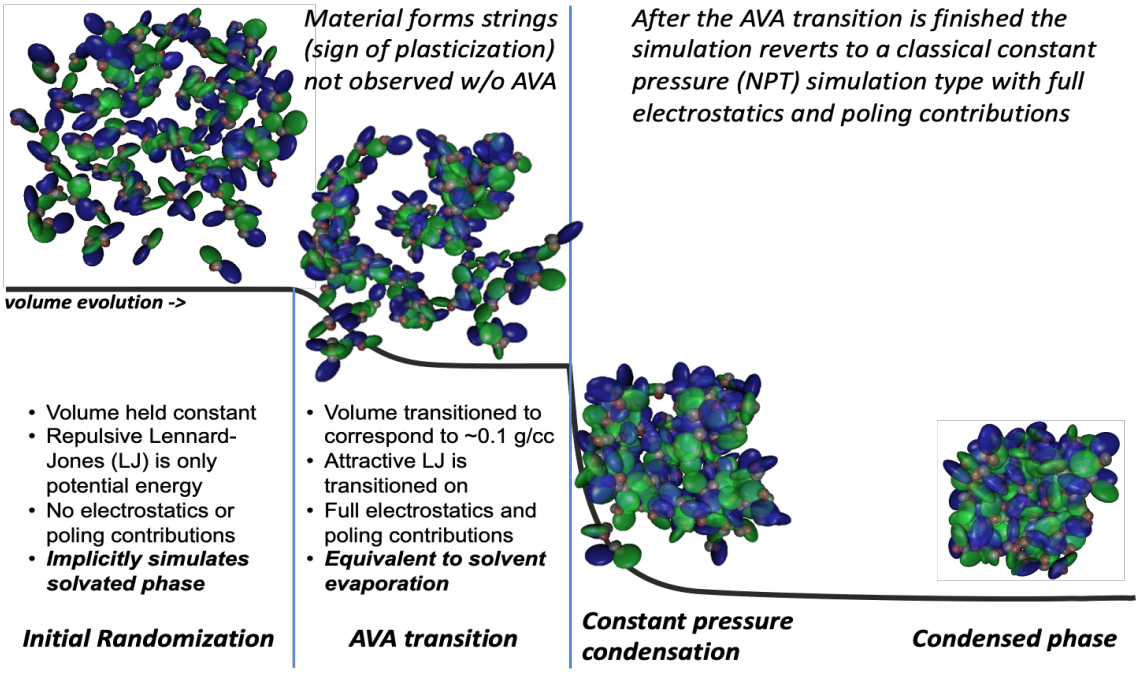

Figure 12. The adiabatic volume adjustment (AVA) computational protocol is illustrated for increasing computational speed and convergence. Figure generated by Dr. Andreas Tillack.

Improved simulations have indicated the difficulty of improving acentric order beyond values of 0.2 for bulk materials when electric field poling is employed. These simulations also indicate the importance of maintaining dipole moments and optical absorption loss within certain ranges. Excessively large dipole moments prevent realizing adequate acentric order. In summary, a wealth of insight is gained from considering simulations of chromophore order under applied forces. It is important to realize that it is $n_e^3 r_{33}$ that is important for electro-optic response. Note that both BAH13 and BAY1 exhibit electro-optic coefficients of 1100 pm/V but the value of $n_e^3 r_{33}$ for BAY1 is 9000 pm/V while that for BAH13 is 7800 pm/V.[92] The values for BAY1 were obtained using TiO_2 charge blocking layers while those for BAH13 were obtained using HfO_2 charge blocking layers.[93] Of course, the optical propagation loss for BAY1 is much higher and limits the utilization of this material.[93] That is, the better optical nonlinearity/optical transparency ratio of BAH13 makes it the material of choice for POH applications. Even greater transparency is required for SOH devices and JRD1 has largely been the material of choice for such devices (although DLD164 has shown comparable results for the shortest waveguide slot widths (electrode separations) of nanophotonic devices).

The problem with respect to electric field poling becomes even more challenging for incorporation of chromophores into nanoscopic devices (see Figures 2 and 14). Theoretical simulations have shown that as slot (electrode spacing) widths, w, are decreased, electro-optic activity is attenuated as shown in Figure 14. Note that theory not only predicts that acentric order is decreased but that centric order transitions from positive to negative values. Negative $\langle\cos^2\theta\rangle$ values indicate that the chromophores are lying down along the electrode surface (orthogonal to the electric field poling direction).

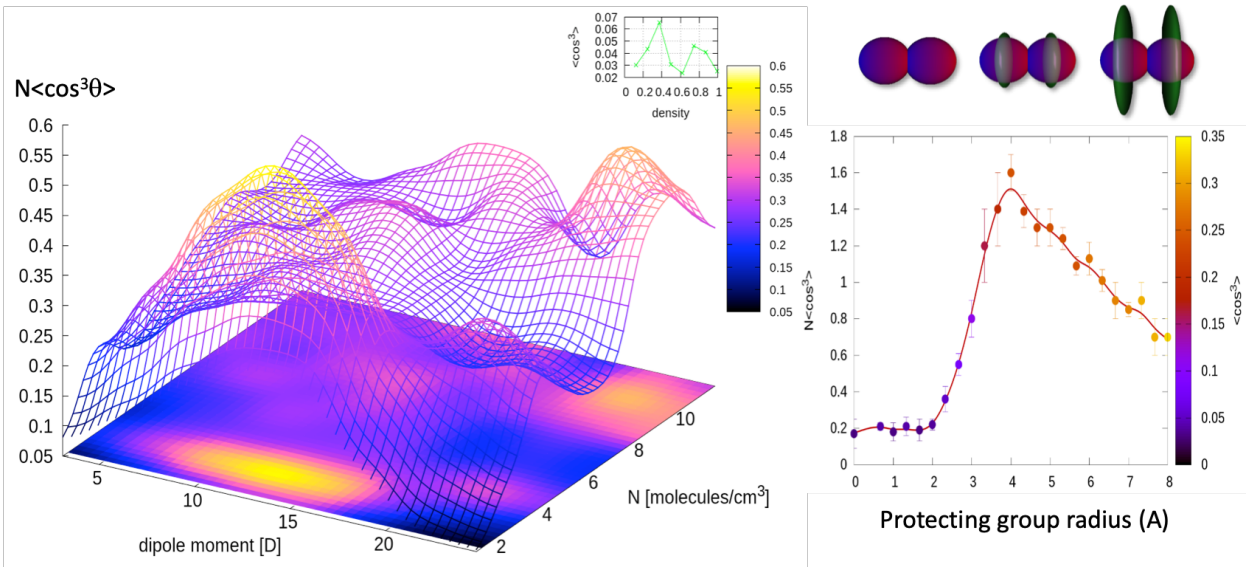

Figure 13. Right: The variation of $N\langle\cos^3\theta\rangle$ (or $\rho_N\langle\cos^3\theta\rangle$) with protecting group radius (in Angstroms, A) is shown. Left: The variation of acentric order ($\langle\cos^3\theta\rangle$ with dipole moment (μ in Debye) and number density (N or ρ_N in molecules per cubic centimeters) is shown. Data for both graphs involve simulations with a LoD = 2. Figure generated by Dr. Andreas Tillack. Adapted from reference 57 with permission.

Chromophores in the vicinity of the gold electrodes introduce "mirror" charges in the conduction electrons of the metal leading to centrosymmetric pairing of chromophores with the mirror charges. Theoretical simulations also explain the effect of reduction of matrix dimensionality on measured $V_\pi L$. The effect is largely through the impact on n_e^3.[90] These calculations illustrate the importance of index of refraction, as well as r_{33}, for improving device performance.

Results for nanoscopic waveguides suggest broadening material processing options from simply electric field poling to also include sequential-synthesis/self-assembly.[3] Covalent coupling of chromophores to an electrode surface provides a means to circumvent attenuation of poling-induced acentric order in the vicinity of electrodes (see Figure 15). Note that acentric order at the electrode surface is essentially zero without covalent coupling restricting chromophores to assume an orientation that is somewhat orthogonal to the electrode surface (see Figure 14). However, consideration of intermolecular dipolar interactions is still important for sequential-synthesis/self-assembly as such interactions cause chromophores to tilt away from the normal to the deposition (electrode) surface. Quantitative simulations of acentric order for chromophores covalently coupled to an electrode surface and to other chromophores in subsequent layers is in a more primitive stage due to the complexity of additional interactions that must be considered. Thus, sequential synthesis is very much still in a basic R&D stage with optimum chromophore assemblies yet to be identified.

Modification of the shape of covalent coupled chromophores is as important in sequential-synthesis/self-assembly as it was for electric field poling. Modification of chromophore moieties to control dipolar interactions is important as shown in Figure 16 where neutral ground state (NGS) and zwitterionic ground state (ZGS) chromophores are covalently coupled to reduce effective dipolar interactions. Such organization permits the electro-optic tensors to constructively add while the dipole moments subtract (point in opposite directions).[169] Other examples of chromophore bundling have been demonstrated.[170,171] Theoretical simulations are required for this processing option and the complexity of the simulations are significantly increased relative to those of electrically poled materials. However, sequential-synthesis/self-assembly affords the possibility of realizing acentric order above 0.2 while also leading to improved thermal and photochemical stability (through the effect of covalent bonds).

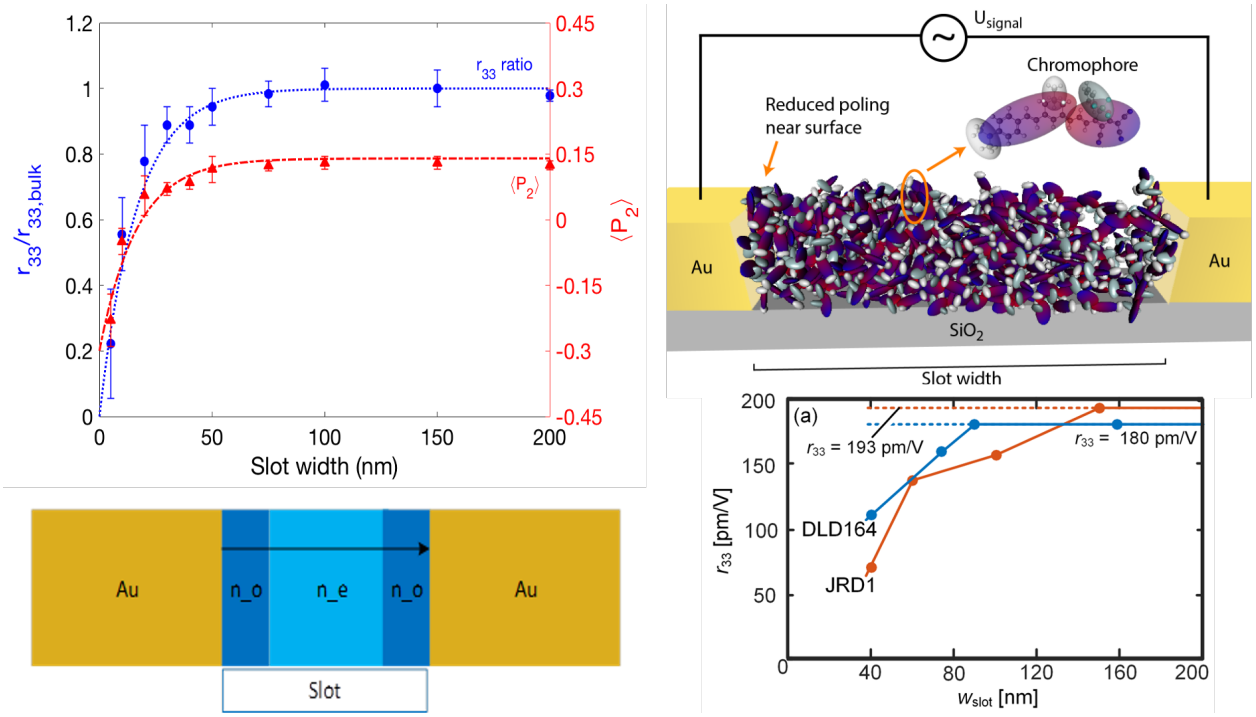

Figure 14. Upper Left: Computer simulation of the variation of electro-optic activity (r_{33} nanophotonic over r_{33} bulk) and centrosymmetric order parameter (P_2) with slot width, w, is shown. Upper Right: A schematic of computed organization of chromophores within the slot is shown for a level-of-detail = 2 chromophore model. Chromophores near the electrodes lie down parallel to the surface due to chromophore/electrode electrostatic interactions. Lower left: A cartoon of the distribution of index of refraction values across the slot is shown. Note near the electrodes, the value is the ordinary index of refraction value, n_o, while in the middle of the slot the value is the extraordinary index of refraction value n_e. Lower Right: Variation of experimental electro-optic coefficient, r_{33}, with w is shown. Adapted from Reference 64 with permission.

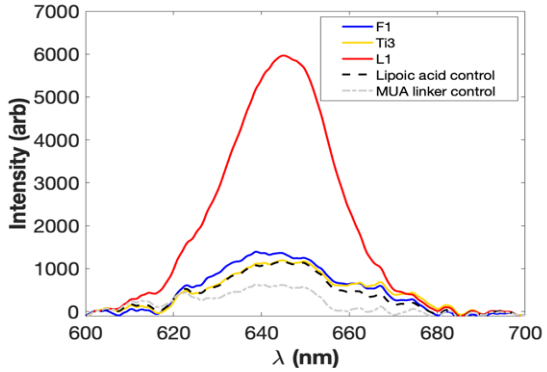

Figure 15. Second harmonic generation from a covalently coupled (to a gold electrode) single chromophore monolayer (strongest signal, L1) is shown together with covalently coupled monolayers that do not contain the chromophore (various controls). This demonstrates that the attenuation of acentric order due to chromophore-electrode interaction can be overcome exploiting the restrictions placed on chromophore movement by covalent bond potentials. Without covalent coupling, chromophores in the monolayer would be oriented parallel to the electrode surface yielding minimum 2nd harmonic signal.

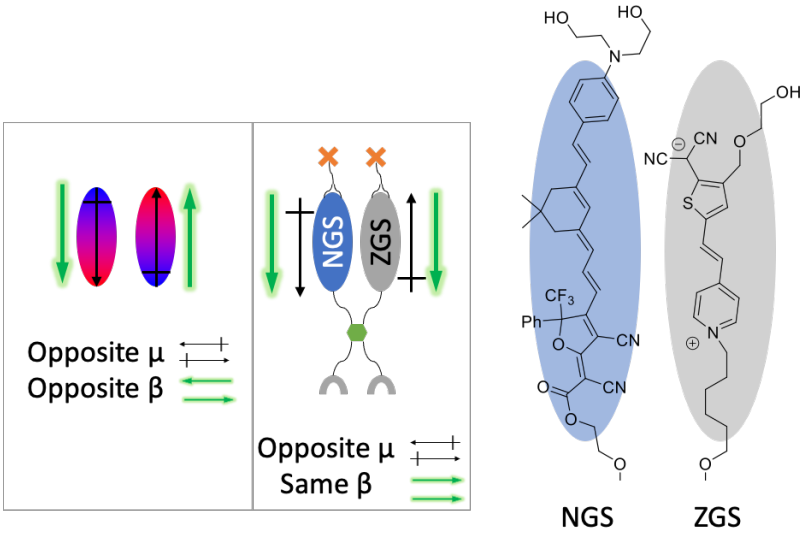

Figure 16. A covalently coupled NGS/ZGS dimer is shown for use with sequential synthesis/self-assembly deposition. Far Left: The situation is shown for two NGS chromophores where centrosymmetric pairing of dipole moments leads to attenuation of β. Middle: the situation is shown for pairing of a ZGS chromophore with a ZGS chromophore, where dipole moments partially cancel but β values add. Far Right: Examples of NGS and ZGS chromophores are given.

In summary, multi-scale (quantum/statistical mechanical) theoretical methods have provided critical guidance for the development of improved materials and processing protocols, including materials and processing methods appropriate for nanophotonic devices. Future exploration of sequential-synthesis/self-assembly methods, including the details of chromophores used for such processing, should lead to significant improvement in device performance and likely affords the best approach to achieving $V_\pi L$ values approaching 1 V-μm (based on the realization of in-device r_{33} values of greater than 1000 pm/V and utilization of electrode separations of < 50 nm). This should dramatically improve the utility of POH devices. Materials prepared by sequential-synthesis/self-assembly also afford improved thermal and photochemical stability and even greater stability can be achieved by lateral crosslinking of such materials.[3] The efficiency of sequential-synthesis/self-assembly processing can be improved using robotic methods and ink jet printing. As already noted, sequential-synthesis/self-assembly processing is not appropriate for large electrode spacings. Thus, electric field poling processing will remain the method of choice for some applications. In like manner, the optical absorption loss of various OEO materials will define their suitability for various applications. In general, OEO materials loss should be equal to or less than the loss associated with passive materials (such as silicon).

3. The Role of Device Architecture on Device Performance.

Critical device performance parameters include drive voltage (and energy efficiency), device optical insertion loss, bandwidth, footprint (device size), stability, and signal linearity[57] (SFDR[57,66,86,100-102] and BER[46,49,52,54,57,61,64,67-69,72,76,78]). The parameters $V_\pi L$ and insertion loss receive the most attention. Optical insertion loss consists of three contributions: (1) Coupling loss, (2) waveguide propagation loss, and (3) material absorption and scattering loss.[3] Most literature discussions focus on propagation loss. One of the most attractive feature of lithium niobate is a very low propagation loss in bulk crystals (i.e., 0.2 dB/cm at telecom wavelengths—the absorption loss is even much lower), which is considerably lower than typical values for OEO materials (i.e., 1-2 dB/cm)[1,3] or of plasmonics and silicon photonics. Silicon waveguides typically exhibit loss values at telecommunication wavelengths on the order of 2 dB/mm, although exact values depend on processing protocols and waveguide architecture. Plasmonic waveguides typically exhibit values between 2 and 6 dB/μm with exact values depending on waveguide dimensions and processing conditions (see Figure 4).[46,87,88] The importance of the contribution of OEO material loss to insertion loss depends on the type of device into which the OEO material is integrated. For example, OEO

material propagation loss at 1.55 μm is often insignificant compared to the propagation loss associated with plasmonic waveguides. Thus, material loss has meaning only in the context of consideration of the type of device being used. Also, high loss can occasionally be overcome by device design. An example of this is provided by work of Haffner coworkers[63] using a combination of passive silicon photonic transmission line waveguides with active integrated plasmonic-organic hybrid ring resonators.[63,87] For this device architecture, the loss of the plasmonic ring modulator comes into play only when the modulator is "on". The loss does not contribute in the "off" state. The ring resonator loss contributes to the desired extinction coefficient and the insertion loss is 1-2 dB.

Coupling loss can be an important and even the dominant contribution to insertion loss in some cases.[1,3] Considerable device engineering has focused on developing efficient couplers including not only between silica and silicon photonic waveguides but also between photonic and plasmonic waveguides (see Figure 17).[1,3,57.61,81]

It is evident that for plasmonic waveguide structures, short electrode lengths are critical because of the high intrinsic propagation loss. For this reason, improvement in $n_e^3 r_{33}$ is important for reducing $V_\pi L$ and thus achieving acceptable V_π and L values. This illustrates the interdependence of materials and device architecture for achieving desired performance. Ideally, $V_\pi L$ should be < 5 V-μm. Short waveguide lengths also facilitate the highest bandwidths. Small $V_\pi L$ values are critical for achieving gain in telecommunication links.

In considering system performance (such as telecommunication systems), a variety of devices must be considered (Figure 17). This is illustrated by a telecommunication testbed developed by our collaborators at the ETH (see Figure 18).[57,65] This includes not only strip-line-type modulators in the transmitter section (such as the IQ modulator shown in Figures 17 and 18) but also resonant electro-optic antennae structures shown in the receiver section of Figure 18. Ring resonators are also commonly utilized electro-optic components.[1,3,12] To this point in time, this testbed has involved use of conventional photodetectors. Ultimately, it may be possible to replace photodetectors based on electron excitation with optical rectification photodetectors based on 2nd order organic NLO materials. Information processing properties such as spur free dynamic range (SFDR)[57] and bit error rate (BER)[57] depend on system properties (and thus on all component properties). The testbed in Figure 18 has been employed to demonstrate performance of telecommunication links and that low noise amplifiers (LNAs) can be eliminated exploiting the gain provided by resonant antenna structures.[50] Elimination of amplifiers is important for optimizing the performance of fiber/wireless telecommunication systems.

Fundamental device architectures can be divided into two categories: (1) strip-line or single pass devices and (2) resonant structures (e.g., ring resonators, Fabry-Perot etalons, photonic crystal devices, etc.) where the optical transmission passes through the device multiple (Q) times.[3,12] This builds up response but at the price of reduced bandwidth. The most common strip-line devices include phase modulators,[40,57] amplitude or Mach Zehnder modulators[48,57,,66,72,75,77], and in-phase-quadrature modulators[43,51,52.57,67,69,88] (see Figure 17). A Mach Zehnder modulator is composed of 2 phase modulators and an IQ modulator is composed of 2 Mach Zehnder modulators.[57,67] These fundamental structures have been used to investigate performance with various modulation protocols[45] [pulse amplitude modulation (PAM)[57,70,77]; non-return to zero (NRZ)[56,70,76]; on-off keying (OOK)[44,76,77]; quadrature amplitude modulation (QAM); quadrature phase shift keying (QPSK)[52,67]; binary phase shift keying (BPSK)[44,57]; polarization shift keying (PoSK); etc.]. 16QAM involves the microwave carrier being modulated into any one of 16 amplitude and phase states.[51,52,57,67,88]

Numerous other device structure relevant to spatial light modulation (optical beam steering)[82-85], RF beam steering[54] (phased array radar), frequency comb generation[37] (see Figure 19), frequency shifting[53], ultra-stable oscillators (and clocks), A/D converters, optical gyroscopes, chemical and physical sensors, etc., have been demonstrated.[3] In most cases, these more complex applications have been realized using the simple device components discussed (e.g., see Figure 19). In all cases, state-of-the-art performance has been demonstrated.

The integration with nanophotonic devices, which has proven so important for OEO materials, has also been exploited for other material classes including lithium niobate (through exploitation of ion-slicing).[172-176] As is to be expected, smaller waveguide dimensions result in some increase in insertion losses. Moreover, $V_\pi L$ values will depend on device architecture and processing conditions. Integration with other materials is not so easily achieved as for OEO material.

Comparison of various EO device technologies is extensively reviewed in the literature.[3,12,17-20,51,52,57,67,77,85,104] Meaningful comparison of different technologies is complex and can be misleading. Some

general comments can be made. Pockels effect devices afford the best signal linearity; electro-absorptive materials suffer from chirp (simultaneous change in both index of refraction and optical absorption that leads to signal distortion). For Pockels materials, signal linearity (SFDR and BER) is determined by the modulator transfer function and thus linearization requires device architecture modification. Electro-absorptive materials suffer from high optical loss (due to optical absorption) and from bandwidth limitations. Inorganic semiconductor materials benefit from the strong semiconductor R&D effort related to electronics.

Basically, plasmonic-organic hybrid (POH) technology affords significant advantages with respect of $V_\pi L$, bandwidth, and energy efficiency but optical propagation loss is a challenge as can be seen from Figure 4. High plasmonic-related loss demands short lengths, which in turn are only possible with high $n_e^3 r_{33}$ materials. In contrast, lithium niobate and silicon-organic hybrid (SOH) afford the advantage of improved optical loss (e.g., $\alpha V_\pi L$ values, where α is propagation loss, are 0.4 VdB for thin film lithium niobate, 1.0 VdB for SOH, and 65 VdB for POH).[77]

As already noted, comparisons of technologies can be misleading. For example, it is device insertion loss, rather than EO material propagation loss, that is important for understanding system performance and this can be dominated by coupling loss or silicon/plasmonic propagation loss rather than EO material loss. Material performance requirements vary widely for different types of devices. For example, for some applications SWaP will be important. In this regard, the $V_\pi L$ metric can be useful. For lithium niobate, $V_\pi L$ ranges from 7 to 5 V-cm achieved with ion-sliced material.[172-176] Silicon-organic hybrid (SOH) devices yield values of 0.5 V-mm, while plasmonic-organic hybrid (POH) devices yield current values of 40-50 V-μm. As evident from Figures 1 and 20, it is important to keep drive voltages to a couple of volts. This limits practical device lengths and can define integration possibilities. Also, drive voltage defines gain that can be achieved in telecommunications systems. Gain (see Figure 20) can typically be achieved for voltages less than 1 volt. Gain is achieved for electrical signals by extracting energy from the optical field and thus a large optical swing is required for a small electrical drive voltage. Note that gain depends on the characteristics of both EO modulators and photodetectors. Introduction of photodetectors based on optical rectification may afford the possibility for improved gain performance.

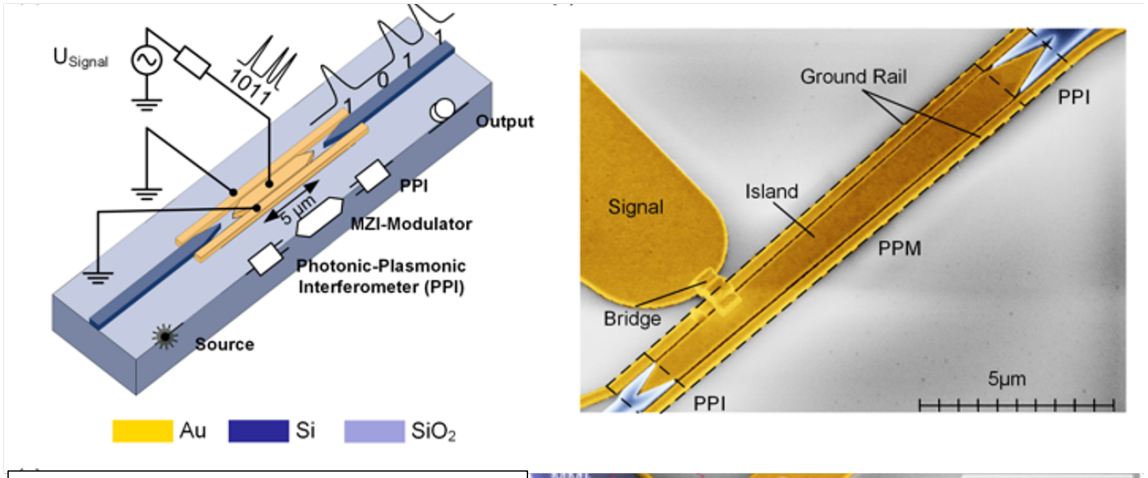

Figure 17. Above Left: A plasmonic phase modulator with photonic-plasmonic transitions is shown.[50] Above Right: A plasmonic Mach Zehnder modulator is shown.[57] Lower Right and Below: A plasmonic in-phase-quadrature (IQ) modulator is shown.[67] Adapted from reference 57 with permission.

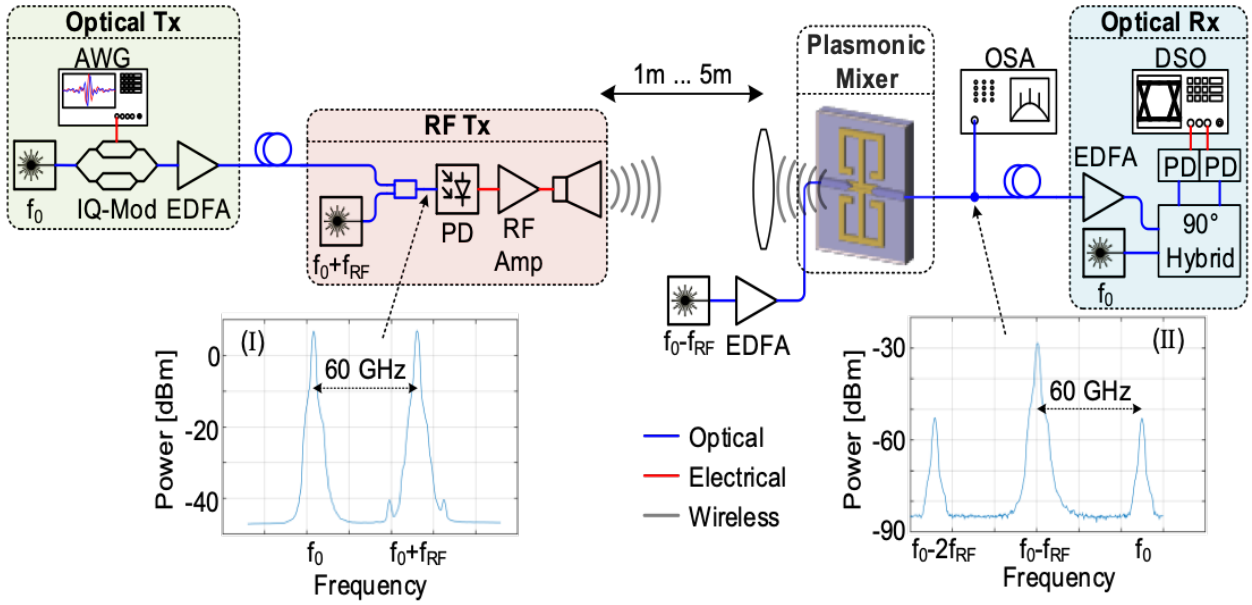

Figure 18. A testbed for modeling fiber/wireless telecommunications is shown. This consists of transmitter (Tx) and receiver (Rx) sections. Electro-optic components consist of an IQ modulator in the transmitter section and a resonant antenna in the receiver section. The high gain of the antenna facilitates elimination of low noise amplifiers in the receiver section. Adapted from reference 65 with permission.

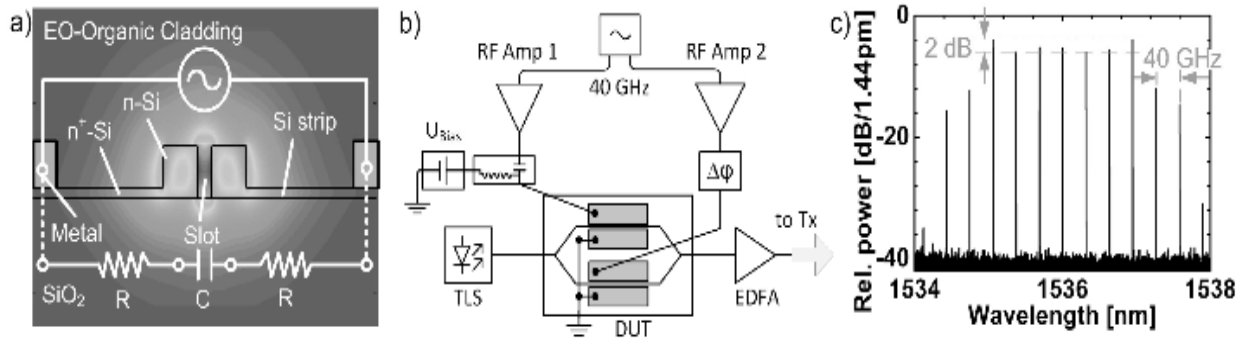

Figure 19. Comb generation based on SOH technology is shown.[37] (a) A cross-sectional view of a SOH phase modulator (one half of the Mach Zehnder modulator) is shown. (b) A schematic of the comb generator is given with the SOH modulators shown in dark grey. (c) The generated comb is shown. Adapted from reference 37 with permission.

Spur free dynamic range (SFDR)[57,66,86,100-102] for analog signal processing and bit error rate (BER)[46,49,52,54,57,61,64,67-69,72,76,78] for digital signal processing depend on several system characteristics and upon the response functions of modulators that define signal linearity. POH and SOH devices yield state-of-the-art SFDR and BER values (see Figure 21 for a graphic definition of and typical performance for SFDR). Further improvement in SFDR requires modulator designs that linearize the response.[100-102] BER depends on the distance over which the signal is propagated but typically POH and SOH devices yield competitive

BER performance and do not require forward error correction (FEC) techniques for shorter propagation distances.[52,57]

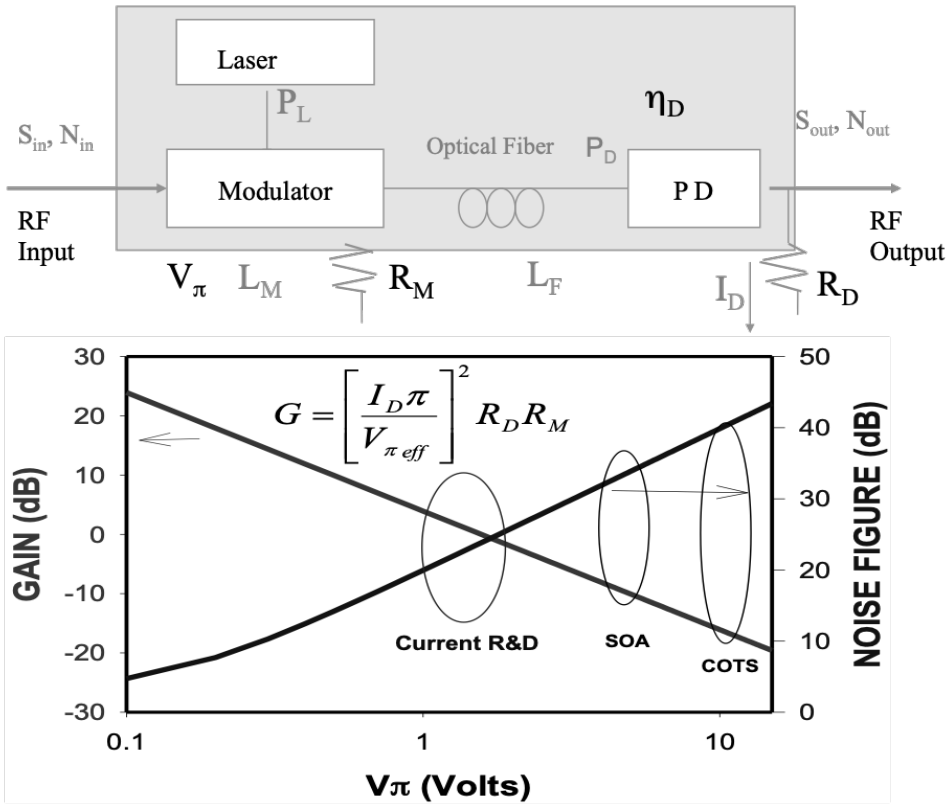

Figure 20. Features that affect gain (G) for a telecommunication link are shown. I_D is detector current and R_D is detector resistance. R_M is modulator resistance. COTS stands for current off-the-shelf (commercial devices), SOA stands for state-of-the-art devices, and current R&D stands for prototype device performance achieved in R&D laboratories.

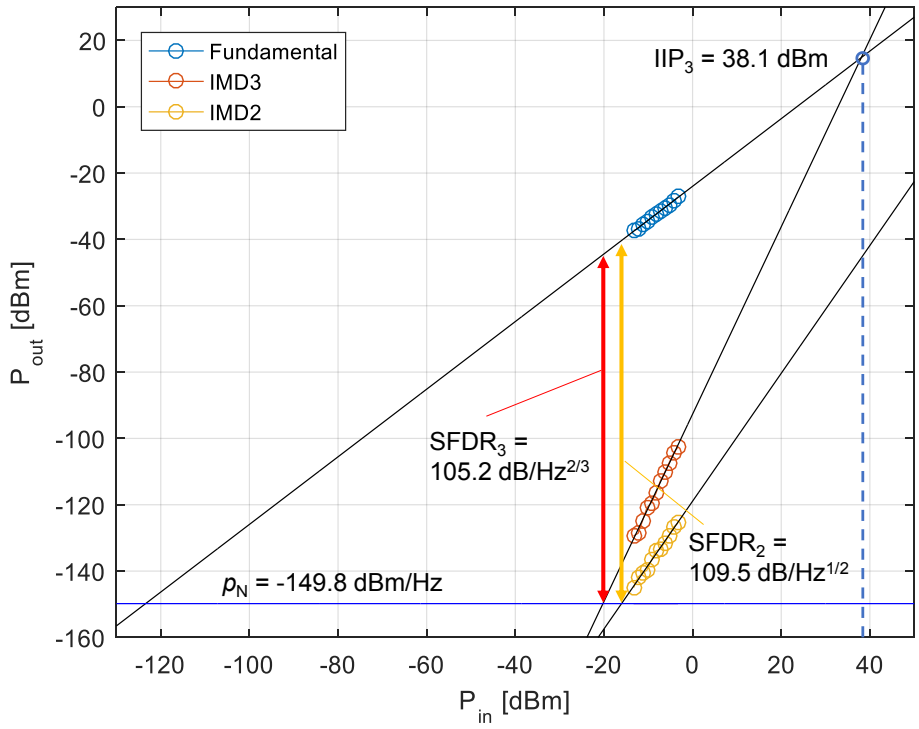

Figure 21. Typical spur free dynamic range (SFDR) for a POH modulator is shown illustrating the definition and determination of SFDR. IMD3 stands for third order intermodulation distortion; IMD2 stands for second order intermodulation distortion. Adapted from references 57, 66, and 86 with permission.

Most of the discussions in this review have focused on guided wave devices. Free space applications, including those based on metasurfaces[82-84], are becoming increasingly important. These can require more complex patterning of materials. Optical loss issues are different, partially due to the shorter optical interaction lengths that can be involved. Thin metasurface devices depend on plasmonic elements for active control of light.

4. Auxiliary Properties, Material Characterization, and Synthetic Methods.

Long term stability of devices is a critical issue.[1,3,89,121,138,177-215] Electrically-poled OEO materials represent a unique challenge in that the poling-induced acentric organization of chromophores is not, in general, thermodynamically stable.[3] Indeed, with increased temperature and time, poling-induced order will be lost. This has been extensively studied and reviewed in many publications.[1,3,89,114,121,138,177-215] It has been well-established that the rate of relaxation can be related to the separation of the measurement temperature (T) from the material glass transition temperature (T_g), i.e., to T-T_g.[3] The dilemma that arises is that one would like to process (i.e., pole) materials at modest temperatures and yet have a final material with the highest possible T_g. This dilemma has been addressed by exploiting crosslinking of OEO chromophores, since T_g is determined by the number of covalent bonds that restrict chromophore movement and by the segmental flexibility of chromophore units.[1,3] Different covalent coupling chemistries have been used to harden chromophore matrices subsequent to the introduction of poling-induced order.[1,3,138,172-204] Cycloaddition reactions, such as the Diels-Alder reaction, are among the most popular as these effect hardening with the least matrix disruption. The elimination products of condensation reactions can disrupt the material matrix both reducing order and increasing optical loss due to scattering.[1,3] Under optimum conditions, very good stability (e.g., T_g > 200°C) can be achieved, although T_g values in the range 150-200°C are more common.[1,3,172-201] Even these lower T_g values are adequate for the production of materials that satisfy Telcordia standards (i.e., long term stability at 85°C).[201] As demonstrated in our 1999 review, this can be accomplished without the introduction of significant scattering loss, i.e., propagation losses on the order of 1 dB/cm can be achieved with some chromophore-containing materials.[1] Thermal relaxation of acentric

order (<cos$^3\theta$>) is typically not a problem for OEO crystals or materials prepared by sequential-synthesis/self-assembly.[3] Thermal relaxation of acentric order does not destroy chromophores and for materials with extensive crosslinking and structure rigidity, very high thermal stability can be achieved. Like optical loss of < 1 dB/cm, such high thermal stability is not easily achieved for potentially viable commercial materials and such performance values are not necessary for most applications.

Irreversible degradation of chromophores most commonly occurs via singlet oxygen chemistry attack on π-electron segments of chromophores.[3,202-204] This has been extensively studied for more than 30 years and has been well-reviewed in the literature.[3,202-204] Dense material matrices tend to inhibit the diffusion of oxygen greatly reducing degradation. With poled materials, stability is improved by packaging of devices (hermetic sealing). In the paint industry, this problem is addressed by addition of singlet oxygen quenchers; this has been demonstrated for electro-optic materials but is not commonly pursued as it is unnecessary to satisfy Telcordia standards. Telcordia standards are easily achieved through matrix hardening (crosslinking) of materials and by encapsulation of devices. The dense matrices of OEO crystals and sequential-synthesis/self-assembly materials greatly inhibit decomposition and stability often exceeds 250°C.

Degradation by high energy radiation is a concern for space applications. OEO materials exhibit excellent stability with respect to high energy radiation and high electric fields due to delocalized electrons rapidly dissipating the localization of charge perturbations.[3,205]

Characterization techniques are critical for understanding material structure/function relationships. These include measurement of electro-optic activity by the Teng-Man[3,206,207] technique, attenuated total reflection (ATR)[3,206], and various device methods such as, for example, Mach Zehnder interferometry[3] (see Figure 22) and index of refraction properties by variable angle spectroscopic ellipsometry (VASE). Thermal properties are measured by thermal gravimetric analysis (TGA) and differential scanning calorimetry (DSC). Centrosymmetric order is measured by variable angle polarization reference absorption spectroscopy (VAPRAS).[111] The characterization of mesoscopic devices is achieved through a variety of techniques most commonly involving the measurement of V_π in devices such as Mach Zehnder interferometers. Characterization of nanoscopic (hybrid POH and SOH) devices has required development of nanophotonic testbeds such as shown in Figure 22.

Each measurement technique has limitations.[3,206] For example, the Teng-Man method[3,206,207] suffers from the need to assume a relationship between r_{33} and r_{13} to extract r_{33} from measurements and large errors can occur from multiple reflection effects. Thus, absolute measurement of r_{33} typically requires alternative techniques such as ATR or Mach Zehnder methods that require more sophisticated fabrication (e.g., electrode deposition) protocols. However, the Teng-Man method is useful for preliminary screening of the relative activity of large numbers of new materials and has the added advantage of *in situ* measurement of poling-induced EO activity, which is important for optimizing poling protocols. It is critical to realize that an important objective in OEO materials research is the timely identification of improved materials. Thus, relative performance, rather than absolute performance, will be important for early stages of development. The final arbitrator of performance is the performance in devices. Thus, relative HRS and Teng-Man measurements have proven useful in identifying chromophores and their associated materials such as BAH13 and JRD1 that yield state-of-the-art performance in POH and SOH devices. Clearly, the evolution from chromophores, to materials, to devices, to systems is a long and complicated one requiring theoretical guidance, numerous characterization measurements, consideration of device architectures, and the requirements of specific applications. Hopefully, this review provides insight into how this complicated development process can be approached in a systematic manner providing access to the literature where greater detail is available.

The synthesis of OEO chromophores and the processing of OEO materials has been reviewed at length elsewhere and will not be repeated here.[3,92,93,121,128-131,134-139,159,160,177-197]

The fabrication and testing of devices have been described in the cited publications related to devices. Fabrication of nanophotonic devices typically involves access to foundry facilities (to be discussed later) and testing requires specialized equipment as can be seen in the following Figure 22. The test bed shown permits evaluation of electro-optic device structures including the systematic variation of device architectures and permits accurate measurement of electro-optic activity.

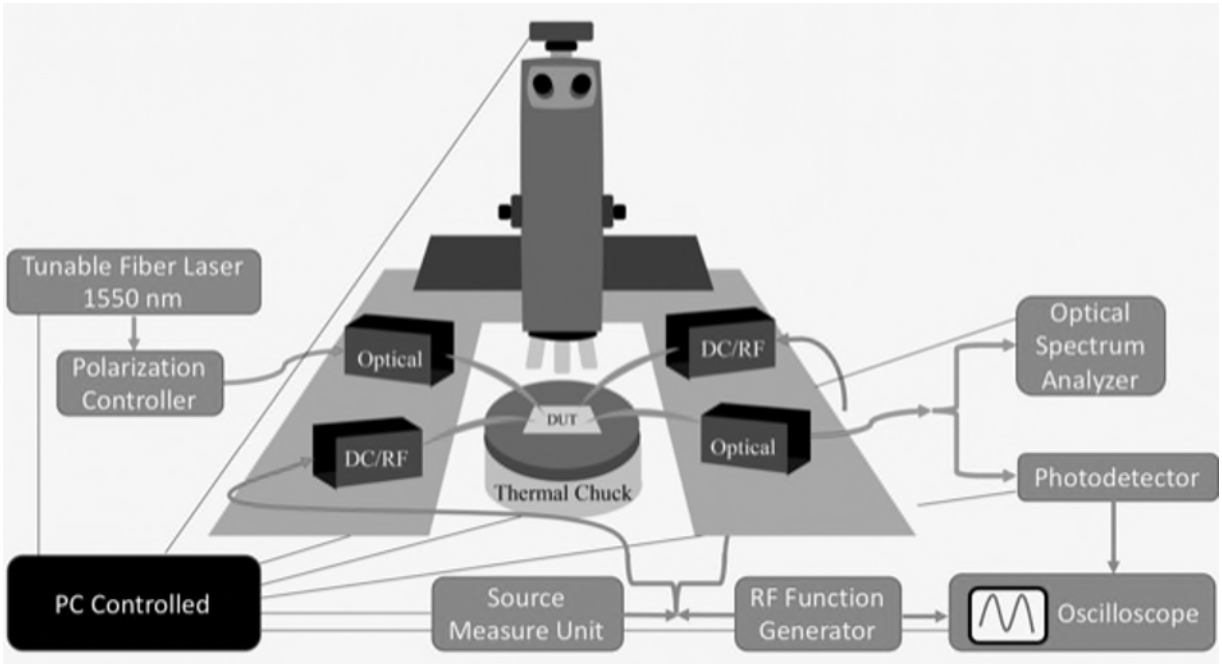

Figure 22. A nanophotonic testbed is shown.

5. Applications and Prognosis.

Applications can be divided into two classes: (1) applications that utilize discrete (single) devices and (2) applications requiring integration of multiple devices (including chip-scale integration of electronic and photonic devices). The former can be found in our earlier review[1,3] while the latter depends on the existence of photonic foundries. Over the past 10 years, more than 35 international foundries and six foundry brokers have come into existence. Pioneering international institutions include Imec (Belgium), CEA Leti (France), IHP (Germany), VTT (Finland), and IME (Singapore and the spin-off company AMF). AIM Photonics and Sandia National Laboratory represent USA foundries among others. The majority of these are focused on silicon photonics although silicon nitride is becoming more frequently considered. Most of these foundries focus on passive photonic circuitry. Foundries that consider OEO materials remain a niche component of the small number of foundries creating active photonic integrated chips (PICs). Our research group has largely relied on the IBM/ETH foundry in Zurich, Switzerland through our ETH collaborators.

Different applications will likely continue to require different materials. For example, discrete device applications, such as optical gyroscopes, that require long pathlengths (and thus low optical loss) will likely continue to be based on low optical loss materials such as silica and lithium niobate. On the other hand, applications that require chip-scale integration of electronics and photonics and photonic device footprints approaching 1 μm^2 will likely favor OEO materials and electro-absorptive materials. Airborne and space telecommunication and some sensor platforms require favorable size, weight, and power (SWAP); these may favor OEO materials that facilitate small, lightweight devices with excellent energy efficiency. SOH technology yields $V_\pi L$ and α characteristics that are intermediate between POH and thin film lithium niobate technologies. If $V_\pi L$ for POH devices can be improved to values approaching 1 V-μm, then the utilization of this technology may expand dramatically. Improvement of POH technology will most likely require a processing paradigm shift to sequential synthesis/self-assembly while electric field poling will continue to be the preferred processing protocol for SOH devices. Sequential synthesis/self-assembly will improve r_{33} and n_e (because of enhanced acentric order) so that $n_e^3 r_{33}$ values more than 10,000 pm/V may be possible. Note that any improvement in $n_e^3 r_{33}$ will also impact SOH and OR devices. Improvement in stability can also be expected with greater covalent bond density. Note that the attenuation of poling efficiency near electrodes is not a critical issue with the wider electrode spacings of SOH devices. Nanoscopic devices will likely prove critical to optical rectification as this appears the only viable route to achieving responsibility values greater than 1 Ampere/Watt for low (MHz) and modest (GHz) frequencies as well as at high (THz)

frequencies; OR is already preferred for high (THz) frequencies as demonstrated by the work of Hayden and others.[5-11]

The application space for electro-optics is broad and rapidly expanding—covering all aspects of information technology. For example, sensor applications are not only far-ranging (covering both physical and chemical sensing) but specific sensor applications such as Lidar are growing in importance.[105-107] Not only has considerable success been demonstrated with respect to environmental imaging and monitoring (as demonstrated by recent National Geographic specials on imaging ancient ruins: https://www.nationalgeographic.com/history/article/maya-laser-lidar-guatemala-pacunam, 11/27/21) but Lidar is now being widely pursued for autonomous vehicles (both ground and airborne) and for applications as far-ranging as agriculture.[105-107]

Of course, the greatest application space for electro-optics likely involves computing (including data centers--datacom) and telecommunications.[203-208] In addition to current fiber and wireless telecommunications, electro-optics is important for supercomputing, quantum computing/quantum communication, and neuromorphic computing. For example, electro-optics can be used to extract information from cryogenic supercomputers to transition information to room temperature photonic transmission. A potential bottleneck for such applications is the need for developing effective photonic foundries capable of complimenting electronic chip foundries and the need to integrate the coordination of such foundries. The emerging technology of optical rectification could have a transformative impact on information technology, but basic research is required to define the noise floor and critical issues related to device architecture and performance. In like manner, hybrid metasurface technology is rapidly evolving and could be significantly important for different aspects of information technology.

Several new companies [Nonlinear Materials Corporation (https://www.nonlinearmaterials.com, 11/27/21), Polariton Technologies (https://www.polariton.ch, 11/27/21), SilOrix GmbH (https://silorix.de, 11/27/21)] have recently been formed to commercialize SOH and POH technologies. Other companies utilizing organic electro-optic materials include Lightwave Logic (https://www.lightwavelogic.com/news/new-release-64/, 1127/21) and Rainbow Photonics AG (http://www.rainbowphotonics.com, 111/27/21). These afford the opportunity to bring together evolving OEO materials and device design/production. Further improvements in material and device architectures will likely be required for effective commercialization. This includes materials other than electro-optic materials, e.g., plasmonic electrodes. Of course, POH and SOH device technologies (and technologies based on integration of OEO materials into metasurfaces) must compete with technologies based on other material classes. Introduction of new materials or improvement of current materials can result in significant changes in capability and market viability. Thus, it is difficult to predict which technologies will be chosen for specific applications; however, the anticipated improvements in POH and SOH technologies may make these very competitive. Unlike electronics and dominant CMOS silicon technology, photonics is far more complex with respect to material and device options. Although the importance of photonic integration has been recognized for more than a decade by Defense Science Board, National Academies, and National Science Foundation workshops and studies, creative R&D remains important for advancing photonic technology and defining choices. Rapidly expanding diverse applications should increase the probability of successful commercialization of POH, SOH, and alternative technologies.

R&D involving materials and device architectures is important as currently no single material or device architecture is ideal for all applications. Ideally, an electro-optic material would have infinite EO activity, no optical absorption or scatting loss, and be infinitely stable at high temperatures and optical powers. Theory-guided R&D has been important for OEO materials and nanophotonic device technologies as it has provided insight on how issues such as the optical nonlinearity/optical transparency trade-off can be improved upon as illustrated in reference 93. The end game has not been realized for OEO materials, plasmonic devices, and silicon photonic devices. Optical loss will continue to be the elephant in the room for all electro-optic technologies and cannot be solved for all applications by materials and device architectures independently. For representative telecommunication waveguide applications, it is important to keep optical insertion loss below 5 dB. This requires keeping the loss associated with both active (EO) and passive materials to appropriate values and keeping coupling losses to within acceptable limits. This will continue to be a challenge for all electro-optic technologies and will often strongly influence the decision to utilize photonics as well as electronics for information technology applications. Device stability is another elephant in the room. Telcordia standards provide the most common guidance with respect to this issue. Early OEO materials clearly did not meet such standards but with lattice hardening (crosslinking) techniques and appropriate packaging, Telcordia standards are now commonly satisfied. This is not sufficient for all

applications. Given that thermal and photochemical stability are directly related to covalent bond density and restriction of motion associated with covalent bonds, theory-guided design of new chromophore materials affords the possibility of further improvement (e.g., sequential-synthesis/self-assembly and crystalline OEO materials provide greater stability). Finally, it is difficult to compete with an establish technology. Lithium niobate has dominated the market for macro/mesoscopic discrete devices[12] and may likely continue to do so but alternative materials may be required for systems requiring nanoscopic devices. While optical loss and stability are dominant concerns, other features such as electro-optic response time (device bandwidth), response linearity, energy efficiency, etc. cannot be ignored. As long as no magic material providing ideal requirements exists, further R&D will be required.

ACKNOWLEDGEMENTS

The authors thank Professor Alvin Kwiram for editing the first draft of this manuscript and for many helpful discussions. The authors thank members of the Dalton/Robinson research group (particularly Drs. Lewis Johnson and Andreas Tillack for their production of crucial theoretical simulations and analysis and for their generation of some of the figures), the Leuthold research group at ETH-Zurich, the Koos research group at Karlsruhe Institute of Technology, and the Clays research group at the University of Leuven for many helpful discussions. The authors also wish to thank the Isborn group for their collaboration and helpful discussions and their generation of a figure. The authors gratefully acknowledge the financial support of the Air Force Office of Scientific Research (FA9550-19-1-0069), National Science Foundation (DMR-13030800, IIP-2036514), the University of Washington College of Arts and Sciences, and a DoD DURIP grant (FA9550-21-1-0193). Part of this work was conducted at the Molecular Analysis Facility, a National Nanotechnology Coordinated Infrastructure (NNCI) site at the University of Washington, which is supported in part by funds from the National Science Foundation (awards NNCI-2025489, NNCI-1542101), the Molecular Engineering & Sciences Institute, and the Clean Energy Institute.

REFERENCES

(1) Dalton, L. R.; Harper, A.; Ren, A.; Wang, F.; Todorova, G.; Chen, J. Zhang, C. Lee, M. Polymeric Electro-Optic Modulators: From Chromophore Design to Integration to Integration with Semiconductor Very Large-Scale Integration Electronics and Silica Fiber Optics. Ind. Eng. Chem. Res. 1999, 38, 8-33, doi: 10.1021/ie9705970.

(2) Pockels, F. Lehrbuch der Kristaloptik 1906, Teubner, Leipzig.

(3) Dalton, L. R.; Gunter, P.; Jabinsek, M.; Kwon. O.-P.; Sullivan, P. A. Organic Electro-Optics and Photonics 2015, Cambridge University Press, Cambridge, UK.

(4) Shi, Y.; Zhang, C.; Zhang, H.; Bechtel, J. H.; Dalton, L. R.; Robinson, B. H.; Steier, W. H. Low (Sub-1 Volt) Halfwave Voltage Polymeric Electrooptic Modulators Achieved by Control of Chromophore Shape. Science 2000, 288(5463), 119-122, doi: 10.1126/science.288.5463.119

(5) Hayden, L. M., Sinyukov, A. M., Leahy, M. R., French, J., Lindahl, P., Herman, W. N., Twieg, R. J., He. M. New Materials for Optical Rectification and Electro-Optic Sampling of Ultrashort Pulses in the Terahertz Regime. J. Polym. Sci. B: Polym. Phys. 2003, 41(21), 2492-2500.

(6) Sinyukov, A. M., Hayden, L. M. Efficient Electrooptic Polymers for THz Applications. J. Phys. Chem. B 2004, 108(25), 8515-8522.

(7) Sinyukov, A. M., Hayden, L. M. Generation and Detection of Terahertz Radiation from Multilayered Electro-Optic Polymer Films. Opt. Lett. 2002, 27(1), 55-57.

(8) McLaughin, C. V., Hayden, L. M., Polishak, B. Huang, S., Luo, J., Kim, T.-D., Jen, A. K.-Y. Wideband 15 THz response Using Organic Electro-Optic Polymer Emitter-Sensor Pairs at Telecommunication Wavelengths. Appl. Phys. Lett. 2008, 92(15), 151107-151107-3.

(9) Sinyukov, A. M., Leahy, M. R., Hayden, L. M., Haller, M., Luo, J., Jen, A. K.-Y., Dalton, L. R. Resonance Enhanced THz Generation in Electro-Optic Polymers Near the Absorption Maximum. Appl. Phys. Lett. 2004, 85(24), 5827-5829.

(10) Leahy-Hoppa, M. R., Fitch, M. J., Zheng, X., Hayden, L. M., Oslander, R. Wideband Terahertz Spectroscopy of Explosives. Chem. Phys. Lett. 2007, 434(4-6), 227-230.

(11) Cunningham, P. D., Valdes, N. N., Vallejo, F. A., Hayden, L. M., Polishak, B. Broadband Terahertz Characterization of the Refractive Index and Absorption of Some Important Polymeric and Organic Electro-Optic Materials. J. Appl. Phys. 109(4), 043505-043505-5.

(12) Chen, A.; Murphy, E. Broadband Optical Modulators: Science, Technology, and Applications 2011, Taylor & Francis, New York, NY.
(13) Almeida, V. R.; Xu, Q.; Barrious, C. A.; Lipson, M. Guiding and Confining Light I Void Nanostructure. Opt. Lett. 2004, 29(11), 1209-1211.
(14) Jalali, B.; Fathpour, S. Silicon Photonics. J. Lightw. Technol. 2006, 24(12), 4600-4615.
(15) Atwater, H. A. The Promise of Plasmonics. Scientific American 2007, 296(4) 56-63.
(16) Schuller, J. A.; Barnard, E. S.; Cai, W. Jun, Y. C.; White, J. S.; Brongersma, M. L. Plasmonics for Extreme Light Concentration and Manipulation. Nat. Mater. 2010, 9(3), 193-204.
(17) Rahim, A.; Hermans, A.; Wohlfeil, B.; Petousi, D.; Kuyken, B.; Van Thourhout, D.; Baets, R. Taking Silicon Photonics Modulators to a Higher Performance Level: State-of-the-Art and a Review of New Technologies. Advanced Photonics 2021, 3(2), 024003-1-23.
(18) Sinatkas, G.; Christopoulos, T.; Tsilpakos, O.; Kriezis, E. Electro-Optic Modulation in Integrated Photonics J. Appl. Phys. 2021, 130, 010901.
(19) Tuniz, A. Nanoscale Nonlinear Plasmonics in Photonic Waveguides and Circuits. La Rivista del Novo Cimento 2021, 44, 193-249.
(20) Gordon, R.; Dobinson, M. Plasmonics-Mine the Gap: Opinion. Optical Materials Express 2021, 11(7), 2192-2196.
(21) Baehr-Jones, T.; Hochberg, M.; Wang, G.; Lawson, R.; Liao, Y.; Sullivan, P. A.; Dalton, L. R.; Jen, A. K.-Y.; Scherer, A. Optical Modulation and Detection in Slotted Silicon Waveguides. Optics Express 2005, 13(14), 5216-5226.
(22) Hochberg, M.; Baehr-Jones, T.; Wang, G.; Shearn, M.; Harvard, K.; Liu, J.; Chen, B.; Shi, Z.; Lawson, R.; Sullivan, P. A.; Jen, A. K.-Y.; Dalton, L. R.; Scherer, A. Terahertz All-Optical Modulation in a Silicon-Polymer Hybrid System. Nat. Mater. 2006, 5(9), 703-709.
(23) Hochberg, M.; Baehr-Jones, T.; Wang, G.; Huang, J.; Sullivan, P. A.; Dalton, L. R.; Scherer, A. Toward a Millivolt Optical Modulator with Nano-Slot Waveguides. Optics Express 2007, 15(13), 8401-8410.
(24) Baehr-Jones, T.; Penkov, B.; Huang, J.; Sullivan, P. A.; Davies, J.; Takayesu, J.; Luo, J.; Kim, T.-D.; Dalton, L. R.; Jen. A. K.-Y.; Hochberg, M.; Scherer, A. Nonlinear Polymer-Clad Silicon Slot Waveguide Modulator with a Half Wave Voltage of 0.25 V. Appl. Phys. Lett. 2008, 92(16), 163303-1-3.
(25) Takayesu, J.; Hochberg, M.; Baehr-Jones, T.; Chan, E.; Wang, G.; Sullivan, P. A.; Liao, Y.; Davies, J.; Dalton, L. R.; Scherer, A.; Krug, W. A Hybrid Electro-Optic Microring Resonator-Based 1x4x1 ROADM for Wafer Scale Optical Interconnects. J. Lightw. Technol. 2008, 27(4), 440-448.
(26) Brosi, J.-M.; Koos, C.; Adnreani, L. C.; Waldow, M.; Leuthold, J.; Freude, W. High-Speed Low-Voltage Electro-Optic Modulator with a Polymer-Infiltrated Silicon Photonic Crystal Waveguide. Optics Express 2008, 16(6), 4177-4191.
(27) Koos, C.; Vorreau, P.; Vlaiatis, T.; Dumon, P.; Bogaerts, W.; Baets, R.; Esembeson, B.; Biaggio, I.; Michinobu, T.; Diederich, F.; Freude, W.; Leuthold, J. All-Optical High-Speed Signal Processing with Silicon-Organic Hybrid Slot Waveguides. Nat. Photon. 2009, 3, 216-219.
(28) Leuthold, J.; Freude, W.; Brosi, J.-M.; Baets, R.; Duman, P.; Biaggio, I.; Scimeca, L.; Diederich, F.; Frank, B.; Koos, C. Silicon Organic Hybrid Technology—A Platform for Practical Nonlinear Optics. Proc. IEEE 2009, 97(7), 1304-1316.
(29) Ding, R.; Baehr-Jones, T.; Liu, Y.; Bojko, R.; Witzen, J.; Su, H.; Luo, J.; Benight, S.; Sullivan, P.; Fedeli, J.-M..; Fournier, M.; Dalton, L. R.; Jen, A.; Hochberg, M. Demonstration of a Low V_pL Modulator with GHz Bandwidth Based on an Electro-Optic Polymer-Clad Silicon Slot Waveguide. Optics Express 2010, 18(15), 15618-15623.
(30) Kim, S.-K.; Slvain, N.; Benight, S.; Kosilkin, I.; Bale, D. H.; Robinson, B. H.; Geary, K.; Jen, A. K.-Y.; Steier, W. H.; Fetterman, H. R.; Berini, P.; Dalton, L. R. Active Plasmonic and Metamaterials and Devices. Proc. SPIE 2010, 7754, 775403-1-10.
(31) Leuthold, J.; Koos, C.; Fruede, W. Nonlinear Silicon Photonics. Nat. Photon. 2010, 4, 535-544.
(32) Figi, H.; Bale, D. H.; Azep, A.; Dalton, L. R.; Chen, A. Electro-Optic Modulation in Horizontally Slotted Silicon/Organic Crystal Hybrid Devices. J. Opt. Soc. Amer. B 2011, 28(9), 2291-2300.
(33) Ding, R.; Baehr-Jones, T.; Kim, W.-J.; Spott, A.; Fournier, M.; Fedeli, J.-M.; Huang, S.; Luo, J.; Jen, A.; Dalton, L. R.; Hochberg, M. Sub-Volt Silicon-Organic Electrooptic Modulator with 500 MHz Bandwidth. J. Lighw. Technol. 2011 29(8), 1112-1117.
(34) Kim, R. S.; Szep, A.; Usechak, G.; Chen, A.; Sun, H.; Shi, S.; Abersinghe, D.; You, Y.-H.; Dalton, L. R. Fabrication and Characterization of a Hybrid 1x4 Silicon-Slot Optical Modulator Incorporating EO Polymers for Optical Phase-Array Antenna Applications. Proc. SPIE 2012 8259, 82590B-1-15.

(35) Dalton, L. R. Theory-Guided Nano-Engineering of Organic Electro-Optic Materials for Hybrid Silicon Photonic, Plasmonic, and Metamaterial Devices. Proc. SPIE 2013, 8622, 86220J-1-10.
(36) Leuthold, J.; Koos, C.; Freude, W.; Alloatti,L.; Palmer, R.; Korn, D.; Pfeifle, J.; Lauermann, M.; Dinu, R.; Wehrli, S.; Jazbinsek, M.; Gunter, P.; Waldow, M.; Whalbrink, T.; Bolten, J.; Kurz, H.; Fournier, M.; Fedeli, J.-M.; Yu, H.; Bogaerts, W. Silicon-Organic Hybrid Electro-Optical Devices. IEEE J. Sel. Top. Quant. Electron. 2013, 19(6), 114-126.
(37) Weimann, C.; Schindler, P. C.; Palmer, R.; Wolf, S.; Bekele, D.; Korn, D.; Pfeifle, J.; Koeber, S.; Schmogrow, R.; Alloatti, L.; Elder, D.; Yu, H.; Bogaerts, W.; Dalton, L. R.; Freude, W.; Leuthold, J.; Koos, C. Silicon-Organic Hybrid (SOH) Frequency Comb Sources for Terabit/s Data Transmission. Optics Express 2014, 22(3) 3629-3647.
(38) Palmer, R.; Koeber, S.; Elder, D. L.; Woessner, M.; Heni, W.; Korn, D.; Lauermann, M.; Bogaerts, W.; Dalton, L. R.; Freude, W.; Leuthold, J.; Koos, C. High-Speed, Low Drive-Voltage Silicon-Organic Hybrid Modulator Based on a Binary-Chromophore Electro-Optic Material. J. Lightw. Technol. 2014, 32(16(, 2726-2734.
(39) Lauermann, M.; Palmer, R.; Koeber, S.; Schindler, P. C.; Wahlbrink, T.; Bolten, J.; Waldow, M.; Elder, D. L.; Dalton, L. R.; Leuthold, J.; Freude, W.; Koos, C. Low-Power Silicon-Organic Hybrid (SOH) Modulators for Advanced Modulation Formats. Optics Express 2014, 22(24), 29927-29936.
(40) Meikyan, A.; Alloatti, L.; Muslja, A.; Hillerkuss, D.; Schindler, P. C.; Li, J.; Palmer, R.; Korn, D.; Muehlbrandt, S.; Van Thourhout, D.; Chen, B.; Dinu, R.; Sommer, M.; Koos, C.; Kohl, M.; Freude, W.; Leuthold, J. High-Speed Plasmonic Phase Modulators. Nat. Photon. 2014, 8, 229-233.
(41) Alloatti, L.; Palmer, R.; Diebold, S.; Pahl, K. P.; Chen, B.; Dinu, R.; Fournier, M.; Fedeli, J.-M.; Zwick, T.; Freude, W.; Koos, C.; Leuthold, J. 100 GHz Silicon-Organic Hybrid Modulator. Light: Sci. & Appl. 2014, 3, e173.
(42) Koeber, S.; Palmer, R.; Lauermann, M.; Heni, W.; Elder, D. L.; Korn, D.; Woessner, M.; Alloatti, L.; Koenig, S.; Schindler, P. C.; Yu, H.; Bogaerts, W.; Dalton, L. R.; Freude, W.; Leuthold, J.; Koos, C. Femtojoule Electro-Optic Modulation Using a Silicon-Organic Hybrid Device. Light: Sci. and Appl. 2015, 4(2), e255.
(43) Lauermann, M.; Wolf, S.; Schindler, P. C.; Palmer, R. Koeber, S.; Korn, D.; Alloatti, L.; Wahlbrink, T.; Bolten, J.; Waldow, M.; Koenigsmann, M.; Kohler, M.; Malsam, D.; Elder, D. L.; Johnston, P. V.; Phillips-Sylvain, N.; Sullivan, P. A.; Dalton, L. R.; Leuthold, J.; Freude, W.; Koos, C. 40 GBd 16QAM Signaling at 160 Gbit/sin a Silicon-Organic Hybrid Modulator. J. Lightw. Technol. 2015, 33(6), 1210-1216.
(44) Meilkyan, A.; Koehnle, K.; Lauermann, M.; Palmer, R.; Koeber, S.; Muenhlbrnadt, S.; Schindler, P. C.; Elder, D. L.; Wolf, S.; Heni, W.; Haffner, C.; Fedoryshyn, Y.; Hillerkuss, D.; Sommer, M.; Dalton, L. R.; Van Thourhout, D.; Freude, W.; Kohl, M.; Leuthold, J. Koos, C. Plasmonic-Organic Hybrid (POH) Modulators for OOK and BPSK Signaling at 40 Gbit/s. Optics Express 2015, 23(8), 9938-9946.
(45) Lauermann, M.; Wolf, S.; Palmer, R.; Koeber, S.; Schindler, P. C.; Wahlbrink, T.; Bolten, J.; Giesecke, A. L.; Koeningsmann, M.; Koehler, M.; Malsam, D.; Elder, D. L.; Dalton, L. R.; Leuthold, J.; Freude, W.; Koos, C. High-Speed and Low Power Silicon-Organic Hybrid Modulators for Advanced Modulation Formats. Proc. SPIE 2015, 9516, 951507-1-5.
(46) Haffner, C.; Heni, W.; Fedoryshyn, Y.; Niegemann, J.; Melikyan, A.; Elder, D. L.; Baeuerle, B.; Salamin, Y.; Josten, A.; Koch, U.; Hoessbacher, C.; Ducry, F.; Juchli, L.; Embroas, A.; Hillerkuss, D.; Kohl, M.; Dalton, L. R.; Hafner, C.; Leuthold, J. All-Plasmonic Mach-Zehnder Modulator Enabling Optical High-Speed Communications at the Microscale. Nat. Photon. 2015, 9(8), 526-528.
(47) Leuthold, J.; Haffner, C.; Heni, W.; Hoessbacher, C.; Niegemann, J.; Fedoryshyn, Y.; Emboras, A.; Hafner, C.; Melikyan, A.; Kohl, M.; Elder, D. L.; Dalton, L.; Tomkos, I. Plasmonic Device for Communications. Optics and Photonics News August 2015, 30-35.
(48) Heni, W.; Haffner, C.; Baeuerle, B.; Fedoryshyn, Y.; Josten, A.; Hillerkuss, D.; Niegemann, J.; Melikyan, A.; Kohl, M.; Elder, D. L.; Dalton, L. R.; Hafner, C.; Leuthold, J. 108 Gbit/s Plasmonic Mach-Zehnder Modulator with > 70 GHz Electrical Bandwidth. J. Lightw. Technol. 2015, 34(2), 393-400.
(49) Heni, W.; Hoessbacker, C.; Haffner, C. Fedoryshyn, Y.; Baeuerle, B.; Josten, A.; Hillerkuss, D.; Salamin, Y.; Bonjour, R.; Melkyan, A.; Kohl, M.; Elder, D. L.; Dalton, L. R.; Hafner, C.; Leuthold, J. High Speed Plasmonic Modulator Array for Enabling Dense Optical Interconnect Solutions. Optics Express 2015, 23(23), 29746-29757.
(50) Salamin, Y.; Heni, W.; Haffner, C.; Fedoryshyn, Y.; Hoessbacher, C.; Bonjour, R.; Zahner, M.; Hillerkuss, D.; Leuchtmann, P.; Elder, D. L.; Dalton, L. R.; Hafner, C.; Leuthold, J. Direct Conversion of

Free Space Millimeter Waves to Optical Domain by Plasmonic Modulator Antenna. Nano Letters 2015, 15(12), 8342-8346.
(51) Koos, C.; Leuthold, J.; Freude, W.; Kohl, M.; Dalton, L. R.; Bogaerts, W.; Giesecke, A. L.; Lauermann, M.; Melikyan, A.; Koeber, S.; Wolf, S.; Weimann, C.; Muehlbrandt, S.; Koehnle, K.; Pfeifle, J.; Hartmann, W.; Kutuvantavida, Y.; Palmer, R.; Korn, D.; Alloatti, L.; Schindler, P. C.; Elder, D. L.; Wahlbrink, T.; Bolten, J. Silicon-Organic Hybrid (SOH) and Plasmonic-Organic Hybrid (POH) Integration. J. Lightw. Technol. 2016, 34(2), 256-268.
(52) Haffner, C.; Heni, W.; Fedoryshyn, Y.; Josten, A.; Baeuerle, B.; Hoessbacher, C.; Salamin, Y.; Koch, U.; Dordevic, N.; Mousel, Bonjour, R.; P.; Emboras, Hillerkuss, D.; Leuchtmann, P.; Elder, D. L.; Dalton, L. R.; Hafner, C.; Leuthold, J. Plasmonic Organic Hybrid Modulators—Scaling Highest-Speed Photonics to the Microscale. IEEE Proc. 2016, 104(12), 2362-2379.
(53) Lauermann, M.; Weimann, C.; Knopf, A.; Heni, W.; Palmer, R.; Koeber, S.; Elder, D. L.; Bogaerts, W.; Leuthold, J.; Dalton, L. R.; Rember, C.; Freude, W.; Koos, C. Integrated Optical Frequency Shifter in Silicon-Organic Hybrid (SOH) Technology. Optics Express 2016, 24(11), 11694-11707.
(54) Bonjour, R.; Burla, M.; Abrecht, F. C.; Welschen, S.; Hoessbacher, C.; Heni W.; Gebrewold, A.; Baeuerle, B.; Josten, A.; Salamin, Y.; Haffner, C.; Johnston, P. V.; Elder, D. L.; Leuchmann, P.; Hillerkuss, D.; Fedoryshyn, Y.; Dalton, L. R.; Hafner, C.; Leuthold, J. Plasmonic Array Feeder Enabling Ultra-Fast Beam Steering at Millimeter Waves. Optics Express 2016, 24(22), 25608-25618.
(55) Heni, W.; Haffner, C.; Elder, D. L.; Fedoryshyn, Y.; Cottier, R.; Salamin, Y.; Hoessbacher, C.; Tillack, A. F.; Robinson, B. H.; Hafner, C.; Dalton, L. R.; Leuthold, J. Nonlinearities of Organic Electro-Optic Materials in Nanoscale Slots and the Implications for the Optimum Modulator Design. Optics Express 2017, 25(3), 2627-2653.
(56) Hoessbacher, C.; Josten, A.; Baeuerle, B.; Fedoryshyn, Y.; Hettrich, H.; Salamin, Y.; Heni, W.; Haffner, C.; Schmid, R.; Elder, D. L.; Hillerkuss, D.; Moller, M.; Dalton, L. R.; Leuthold, J. Plasmonic Modulator with > 170 GHz Bandwidth Demonstrated at 100 Gbit/s NRZ. Optics Express 2017, 25(3), 1762-1768.
(57) Heni, W.; Kutuvantavida, Y.; Haffner, C.; Zwickel, H.; Kieninger, C.; Wolf, S.; Lauermann, M.; Tillack, A.; Johnson, L. E.; Elder, D. L.; Robinson, B. H.; Freude, W.; Koos, C.; Leuthold, J.; Dalton, L. R. Silicon-Organic and Plasmonic-Organic Hybrid Photonics. ACS Photonics 2017, 4(7), 1578-1590.
(58) Koos, C.; Freude, W.; Leuthold, J.; Dalton, L. R.; Wolf, S.; Muenhlbrandt, S.; Melikyan, A.; Zwickel, H.; Harter, T.; Kutuvantavida, Y.; Kieninger, C.; Lauermann, M.; Elder, D. Nanophotonic Modulators and Photodectors Using Silicon Photonic and Plasmonic Device Concepts. Proc. SPIE 2017, 10098, 1009807.
(59) Hoessbacher, C.; Salamin, Y.; Fedoryshyn, Y.; Heni, W.; Josten, A.; Baeuerle, B.; Haffner, C.; M. Zahner, Chen, H.; Elder, D. L.; Wehrli, S.; Hillerkuss, D.; Van Thourhout, D.; Van Campenhout, J.; Dalton, L. R.; Hafner, C.; Leuthold, J. Optical Interconnect Solution with Plasmonic Modulator and Germanium Photodetector Array. IEEE Photon. Technol. Lett. 2017, 29(21), 1760-1763.
(60) Haffner, C.; Heni, W.; Dordevic, N.; Chaelladurai, D.; Elder, D. L.; Fedoryshyn, Y.; Portner, K.; Burla, M.; Robinson, B. H.; Dalton, L. R.; Leuthold, J. Harnessing Nonlinearities near Material Absorption Resonances for Reducing Losses in Plasmonic Modulators. Optical Materials Express 2017, 7(7), 2168-2181.
(61) Ayata, M.; Fedoryshyn, Y.; Heni, W.; Baeuerle, B.; Josten, A.; Elder, D. L.; Dalton, L. R.; Leuthold, J. Complete High-Speed Plasmonic Modulator in a Single Metal Layer. Science 2017, 358(6363), 630-632.
(62) Kieninger, C.; Kutuvantavida, Y.; Elder, D. L.; Wolf, S.; Zwickel, H.; Blaicher, M.; Kemal, J. N.; Lauermann, M.; Randel, S.; Freude, W.; Dalton, L. R.; Koos, C. Ultra-High Electro-Optic Activity Demonstrated in a Silicon-Organic Hybrid Modulator. Optica 2018, 5(6), 739-748.
(63) Haffner, C.; Chelladurai, D.; Fedoryshyn, Y.; Baeuerle, B.; Josten, A.; Heni, W.; Cui, T.; Saha, S.; Elder, D. L.; Dalton, L. R.; Boltasseva, A.; Shalaev, V.; Kinsey, N.; Leuthold, J. Low Loss Plasmon-Assisted Electro-Optic Modulator. Nature 2018, 556(7702), 483-486.
(64) Robinson, B. H.; Johnson, L. E.; Elder, D. L.; Kocherzhenko, A. A.; Isborn, C. M.; Haffner, C.; Heni, W.; Hoessbacher, C.; Fedoryshyn, Y.; Salamin, Y.; Baeuerle, B.; Josten, A.; Ayata, M.; Koch, U.; Luethold, J.; Dalton, L. R. Optimization of Plasmonic-Organic Hybrid Electro-Optics. J. Lightw. Technol. 2018, 36(21), 5036-5047.
(65) Salamin, C.; Baeuerle, B.; Heni, W.; Abrecht, F. C.; Josten, A.; Fedoryshyn, Y.; Haffner, C.; Bonjour, R.; Watanabe, T.; Burla, M.; Elder, D. L.; Dalton, L. R.; Leuthold, J. Microwave Plasmonic Mixer in a Transparent Fibre-Wireless Link. Nat. Photon. 2018, 12, 749-753.

(66) Burla, M.; Hoessbacher, C.; Heni, W.; Haffner, C.; Fedoryshyn, Y.; Werner, D.; Watanabe, T.; Massler, H.; Elder, D. L.; Dalton, L. R.; Leuthold, J. 500 GHz Plasmonic Mach-Zehnder Modulator Enabling Sub-THz Microwave Photonics. APL Photonics 2019, 4(5), 056106.
(67) Heni, W.; Fedoryshyn, Y.; Baeuerle, B.; Josten, A.; Hoessbacher, C.; Messner, A.; Haffner, C.; Watanabe, Salamin, Y.; Koch, U.; Elder, D. L.; Dalton, L. R.; Leuthold, J. Plasmonic IQ-Modulators with Atto-Joule/Bit Electrical Energy Consumption. Nat. Commun. 2019, 10(1), 1694-1702.
(68) Koch, U.; Messner, A.; Hoessbacher, C.; Heni, W.; Josten, A.; Baeuerle, B.; Ayata, M.; Fedoryshyn, Y.; Elder, D. L.; Dalton, L. R.; Leuthold, J. Ultra-Compact Plasmonic Modulator Array. J. Lightw. Technol. 2019, 37(5), 1484-1491.
(69) Ayata, M.; Fedoryshyn, Y.; Heni, W.; Josten, A.; Baeuerle, B.; Haffner, C.; Hoessbacher, C.; Koch, U.; Salamin, Y.; Elder, D. L.; Dalton, L. R.; Leuthold, J. All-Plasmonic IQ Modulator with a 36 nm Fiber-to-Fiber Pitch. J. Lightw. Technol. 2019, 37(5), 1492-1497.
(70) Baeuerle, B.; Heni, W.; Hoessbacher, C.; Fedoryshyn, Y.; Josten, A.; Haffner, C.; Watanabe, T.; Uhl, C.; Hettrich, H.; Elder, D. L.; Dalton, L. R.; Moller, M.; Leuthold, J. Reduced Equalization Needs of 100 GHz Bandwidth Plasmonic Modulators. J. Lightw. Technol. 2019, 37(9), 2050-2057.
(71) Burla, M.; Salamin, Y.; Bonjour, R.; Abrecht, F.; Hoessbacher, C.; Haffner, C.; Heni, W.; Fedoryshyn, Y.; Werner, D.; Baeuerle, B.; Josten, A.; Watanabe, T.; Hillerkuss, D.; Elder, D. L.; Dalton, L.; Leuthold. Integrated Photonic and Plasmonic Technologies for Microwave Signal Processing Enabling mm-Wave and Sub-THz Wireless Communication Systems. Proc. SPIE 2019, 10945, 1094505.
(72) Baeuerle, B.; Heni, W.; Hoessbacher, C.; Fedoryshyn, Y.; Koch, U.; Josten, A.; Watanabe, T.; Uhl, C.; Hettrich, H.; Elder, D. L.; Dalton, L. R.; Moller, M.; Leuthold, J. 120 GBd Plasmonic Mach-Zehnder Modulator with a Novel Differential Electrode Design Operated at a Peak-to-Peak Drive Voltage of 178 mV. Optics Express 2019, 27(12), 16823-16832.
(73) Salamin, Y.; Benea-Chelmus, I.-C.; Fedoryshyn, Y.; Heni, W.; Elder, D. L.; Dalton, L. R.; Faist, J.; Leuthold, J. Compact and Ultra-Efficient Broadband Plasmonic Terahertz Field Detector. Nat. Commun. 2019, 10(1), 5530.
(74) Koch, U. Uhl, C.; Hettrich, H.; Fedoryshyn, Y.; Hoessbacher, C.; Heni, W.; Baeuerle, B.; Bitachon, B.; Josten, A.; Ayata, M.; Xu, H.; Elder, D. L.; Dalton, L. R.; Mentovich, E.; Bakopoulos, P.; Zimmermann, L.; Tsiokos, D.; Pieros, N.; Moller, M.; Leuthold, J. A Monolithic BiCMOS Electronic-Plasmonic High-Speed Transmitter. Nat. Electron.2020, 3, 338-345.
(75) Benea-Chelmus, I.-C.; Salamin, Y.; Settembrini, F. F.; Fedoryshyn, Y.; Heni, W.; Elder, D. L.; Dalton, L. R.; Leuthold, J. Electro-Optic Coherent Interface for Ultra-Sensitive Time-Domain Cavity Quantum Electrodynamics Experiments from Microwave to Terahertz Frequencies. Optica 2020, 7(5), 498-505.
(76) Baeuerle, B.; Hoessbacher, C.; Heni, W.; Fedoryshyn, Y.; Koch, U.; Josten, A.; Elder, D. L.; Dalton, L. R.; Leuthold, J. 100 GBd IM/DD Transmission over 14 km SMF in the C-Band Enabled by a Plasmonic SSB MZM. Optics Express 2020, 28(6), 8601-8608.
(77) Kieninger, C.; Fullner, C.; Zwickel, H.; Kutuvantavida, Y.; Kemal, J. N.; Eschenbaum, C.; Elder, D. L.; Dalton, L. R.; Freude, W.; Randel, S.; Koos, C. Silicon-Organic Hybrid (SOH) Mach-Zehnder Modulators for 100 GBd PAM4 Signaling with Sub-1 dB Phase-Shifter Loss. Optics Express 2020, 28(17), 24693-24707.
(78) Heni, W.; Baeuerle, B.; Mardoyan, H.; Jorge, F.; Estaran, J. M.; Konczykowska, A.; Riet, M.; Duval, B.; Bordjiadjim, B.; Goix, M.; Dupuy, J.-Y.; Destraz, M.; Hoessbacher, C.; Fedoryshyn, Y.; Xu, H.; Elder, D. L.; Dalton, L. R.; Renaudier, J.; Leuthold, J. Ultra-High-Speed 2:1 Digital Selector and Plasmonic Modulator IM/DD Transmitter Operating at 222 GBaud for Intra-Datacenter Applications. J. Lightw. Technol. 2020, 38(9), 2734-2739.
(79) Ummethala, S.; Kermal, J. N.; Alam, A. S.; Lauermann, M.; Kutuvantavida, Y.; Nandam, S. H.; Hahn, L.; Elder, D. L.; Dalton, L. R.; Zwick, T.; Randel, S.; Freude, W.; Koos, C. Hybrid Electro-Optic Modulator Combining Silicon Photonic Slot Waveguides with High-k Radio-Frequency Slotlines. Optica 2020, 8(4), 511-519.
(80) Ma, P.; Salamin, Y.; Messner, A.; Baeuerle, B.; Embroas, A.; Heni, W.; Josten, A.; Eltes, F.; Abel, S.; Formpeyrine, J.; Elder, D. L.; Dalton, L. R.; Leuthold, J. Plasmonic Modulators and Photodetectors for Communications. Proc. SPIE 2021, 11711, 11711O5.
(81) Messner, A.; Jud, P. A.; Winiger, J.; Eppenberger, M.; Chelladurai, D.; Heni, W.; Baeuerle, B.; Koch, U.; Ma, P.; Haffner, C.; Xu, H.; Elder, D. L.; Dalton, L. R.; Smajic, J.; Leuthold, J. Broadband Metallic Fiber-to-Chip Couplers and a Low-Complexity Integrated Plasmonic Platform. Nano Lett. 2021, 21(11), 4539-4545.

(82) Benea-Chelmus, I.-C.; Meretska, M.; Tamagnone M.; Elder, D. L.; Dalton, L. R.; Capasso, F. Electrically Tunable Metasurfaces by a Single Electro-Optic Layer. Proc. SPIE 2021, 11682, 11682-1-11.
(83) Benea-Chelmus, I.-C.; Meretska, M.; Elder, D. L.; Dalton, L. R.; Capasso, F. Mie-Driven Free-Space Electro-Optic Transducers. Proc. SPIE 2021, 11796, 117969V.
(84) Benea-Chelmus, I.-C.; Meretska, M.; Elder, D. L.; Tamagnone, M.; Dalton, L. R.; Capasso, Electro-Optic Spatial Light Modulator from an Engineered Organic Layer. Nat. Commun. 2021, 12. 5928, https://doi.org/10.1038/s41467-021-26035-y.
(85) Koch, U.; Uhl, C.; Hettrich, H.; Fedoryshyn, Y.; Moor, D.; Baumann, M.; Hoessbacher, C.; Heni, W.; Baeuerle, B.; Bitachon, Bertold, Josten, A.; Ayata, M.; Xu, H.; Delwin, D. L.; Dalton, L. R.; Mentovich, E.; Bakopoulos, P.; Lischke, S.; Kruger, A.; Zimmermann, L.; Tsiokos, D.; Pleros, N.; Moller, M.; Leuthold, J. Plasmonics—High-Speed Photonics for Co-Integration with Electronics. Japanese Journal of Applied Physics 2021, 60, SB0806.
(86) Burla, M.; Hoessbacher, C.; Heni, W.; Haffner, C.; Fedoryshyn, Y.; Werner, D.; Watanabe, T.; Salamin, Y.; Massler, H.; Hillerkuss, D.; Elder, D.; Dalton, L.; Leuthold, J. Novel Applications of Plasmonics and Photonics Devices to Sub-THz Wireless. Proc. SPIE 2020, 11307, 113070I, doi.org/10.1117/12.2550323.
(87) Haffner, C. Non-Resonant and Resonant Surface Plasmon Polariton Modulators for Optical Communications 2018, Ph.D. Dissertation No. ETH 25089, ETH Zurich Series in Electromagnetic Fields, Vol. 6. 1-215.
(88) Ummethala, S. Plasmonic-Organic and Silicon-Organic Hybrid Modulators for High-Speed Signal Processing. Dr.-Ing. Dissertation. 2021. KIT-Fakultat fur Electrotechnik und Informationstecknik des Karlsruher Instituts fur Technologie (KIT), 1-164.
(89) Johnson, L. E.; Elder, D. L.; Xu, H.; Hammond, S. R.; Benight, S. J.; O'Malley, K.; Robinson, B. H.; Dalton, L. R. New Paradigms in Materials and Devices for Hybrid Electro-Optics and Optical Rectification. Proc. SPIE 2021, 11812, 1181292.
(90) Johnson, L. E.; Elder, D. L.; Benight, S. J.; Tillack, A. F.; Hammond, S. R.; Heni, W.; Dalton, L. R.; Robinson, B. H. Birefringence, Dimensionality, and Surface Influences on Organic Hybrid Electro-Optic Performance. Proc. SPIE 2021, 11799, 1179917.
(91) Baehr-Jones, T.; Witzens, J.; Hochberg, M. Theoretical Study of Optical Rectification at Radio Frequencies. IEEE J. Quant. Electron. 2010, 46(11), 1634-1641.
(92) Xu, H.; Elder, D. L.; Johnson, L. E.; de Coene, Y.; Hammond, S. R.; Vander Ghinst, W.; Clays, K.; Dalton, L. R.; Robinson, B. H. Electro-Optic Activity in Excess of 1000 pm/V Achieved via Theory-Guided Organic Chromophore Design. Adv. Mater. 2021, 333(45) 2104174 published on-line at https://doi.org/10.1002/adma.202104174.
(93) Xu, H.; Elder, D. L.; Johnson, L. E.; Heni, W.; de Coene, Y.; Leo, de Leo, E.; Destraz, M.; Meier, N.; Vander Ghinst, W.; Hammon, S. R.; Clays, K.; Leuthold, J.; Dalton, L. R.; Robinson, B. H. Theory-Guided Design and Synthesis of Chromophores with Enhanced Electro-Optic Activities in Both Bulk and Plasmonic-Organic Hybrid Devices. Materials Horizons 2021, published online at https://pubs.rsc.org/en/content/articlelanding/2021/mh/d1mh01206a.
(94) Cox, C. H., Wooten, E. L. Photodetection Via Optical Rectification of Terahertz-Modulated Optical Carriers. J. Lightw. Technol. 2021, 39(24), 7908-7914.
(95) Facchetti, A.; Abbotto, A.; Beverina, L.; Van der Boom, M.; Dutta, P.; Evmenenko, G.; Pagani, G. A., Marks, T. J. Layer-by-Layer Self-Assembled Pyrrole-Based Donor-Acceptor Chromophores as Electro-Optic Materials. Chem. Mater. 2003, 15(5), 1064-1072.
(96) Facchetti, A.; Abbotto, A.; Beverina, L.; Bradamante, S.; van der Boom, M. E.; Evmenenko, G.; Dutta, P.; Marks, T. J.; Pagani, G. A. Azinium-(p-Bridge)-Pyrrole NLO-Phores: Influence of Heterocycle Acceptors on Chromophoric and Self-Assembly Thin-Film Properties. Chem. Mater. 2002, 14, 4996-5005.
(97) Zhao, Y. G.; Wu, A.; Lu, J. L.; Chang, S.; Lu, W. K.; Ho, S. T.; Van der Boom, M. E.; Marks, T. J. Traveling Wave Electro-Optic Phase Modulators Based on Intrinsically Polar Self-Assembled Chromophoric Superlattices. Appl. Phys. Lett. 2001, 79(5), 587-589.
(98) Lin, W.; Lin, W.; Wong, G. K.; Marks, T. T. Supramolecular Approaches to Second-Order Nonlinear Optical Materials. Self-Assembly and Microstructural Characterization of Intrinsically Acentric [(Aminophenyl)azo]pyridinium Superlattices. J. Am. Chem. Soc. 1996, 118, 8034-8042.
(99) Roscoe, S. B.; Yitzchaik, S.; Kakkar, A. K.; Marks, T. J.; Xu, Z.; Zhang, T.; Lin, W.; Wong, G. K. Self-Assembled Chromophore NLO-Active Structures. Second-Harmonic Generation and X-Ray Photoelectron

Spectroscopic Studies of Nucleophilic Substitution and Ion Exchange Processes on Benzyl Halide-Functionalized Surfaces. Langmuir 1996, 12(22), 5338-5349.
(100) Ackerman, E. I. Broad-band Linearization of a Mach-Zehnder Electrooptic Modulator. IEEE Transactions on Microwave Theory and Techniques. 1999, 47(12), 2271-2279.
(101) Gill, D. M.; Rasras, M.; Tu, K.-Y.; Chen, Y.-K.; White, A. E.; Patel, S.; Carothers, D.; Pomerene, A.; Kamocsai, R.; Beattie, J.; Kopa, A.; Apsel, A.; Beals, M.; Mitchel, J.; Liu, J.; Kimerling, L. C. Optical Modulation Techniques for Analog Signal Processing and CMOS Compatible Electrooptic Modulation. Proc. SPIE 2008, 6898, 689803-11.
(102) Zhu, X.; Jin, T.; Chi, H.; Zhou, J.; Tong, G.; Li, D.; Zuo, L.; Fu, Y. Linearization of Two Cascaded Intensity-Modulator-Based Analog Photonic Link. Proc. SPIE 2018, 57(8), 080501.
(103) Amin, R.; Maiti, R.; Gui, Y.; Suer, C.; Miscuglio, M.; Heidari, E.; Chen, R. T.; Dalir, H.; Sorger, V. J. Sub-Wavelength GHz-Fast Broadband ITO Mach-Zehnder Modulator on Silicon Photonics. Optica 2020, 7(4), 333-335.
(104) Marpaung, D.; Roeloffzen, C; Heideman, R.;; Leinse, A.; Sales, S.; Capmany, J. Integrated Microwave Photonics. Laser& Photonics Reviews 2013, 7(4). 506-538.
(105) Verghese, S. Self-Driving Cars and Lidar. Conference on Lasers and Electro-Optics, OSA Technical Digest (online) 2017, paper AM3A.1.
(106) Hudnut, K. W.; Brooks, B. A.; Scharer, K.; Hernandez, J. L.; Dawson, T. E.; Oskin, M. E.; Arrowsmith, J. R.; Goulet, C. A.; Blake, K.; Boggs, M. L.; Bork, S.; Glennie, C. L.; Fernandez-Diaz, J. C.; Singhania, A.; Hauser, D.; Sorhus, S. Airborne Lidar and Electro-Optical Imagery Along Surface Ruptures of the 2019 Ridgecrest Earthquake Sequence, Southern California. Seismological Research Letters 2020, 91(4), 2996-2107.
(107) https://www.electrooptics.com/tags/environmental-monitoring, 11/28/21.
(108) Pan, S.; Zhang, Y. Microwave Photonic Radars. J. Lightw. Technol. 2020, 38(19), 5450-5484.
(109) Morris, T. A.; Wheeler, J. M.; Grant, M. J.; Digonnet, M. J. F. Advances in Optical Gyroscopes. Proc. SPIE 2019, 11199, 11199OT.
(110) Olbricht, B. C.; Sullivan, P. A.; Wen, G.-A.; Mistry, A.; Davies, J. A.; Ewy, T. R.; Eichinger, B. E.; Robinson, B. H.; Reid, P. J.; Dalton, L. R. Laser-Assisted Poling of Binary Chromophore Materials. J. Phys. Chem. C 2008, 112, 7983-7988.
(111) Olbricht, B. S.; Sullivan, P. A.; Davies, J. A.; Dennis, P. C.; Hurst, J. T.; Johnson, L. E.; Bale, D. H.; Benight, S. J.; Hilfiker, J. N.; Chen, A.; Eichinger, B. E.; Reid, P. J.; Dalton, L. R.; Robinson, B. H. Measuring Order in Contact-Poled Organic Electro-Optic Materials with Variable Angle Polarization-Referenced Absorption Spectroscopy (VAPRAS). J. Phys. Chem. B 2011, 115, 231-241.
(112) Marder, S. R.; Gorman, G. B.; Meyers, F.; Perry, J. W.; Bourhill, G.; Bredas, J. L.; Pierce, B. M. Unified Description of Linear and Nonlinear Polarizations in Organic Polymethine Dyes. Science 2004, 265, 632-635.
(113) Meyers, F.; Marder, S. R.; Pierce, B. M.; Bredas, J. L. Electric-Field Modulated Nonlinear Optical Properties of Donor-Acceptor Polyenes: Sum-Over-States Investigation of the Relationship Between Molecular Polarizabilities (Alpha, Beta, and Gamma) and Bond-Length Alternation. J. Am. Chem. Soc. 1994, 116, 10703-10714.
(114) Bourhill, G.; Bredas, J. L.; Cheng, L.-T.; Marder, S. R.; Meyers, F.; Perry, J. W.; Tiemann, R. G. Experimental Demonstration of the Dependence of the First Hyperpolarizability of Donor-Acceptor-Substituted Polyenes on the Ground-State Polarization and Bond-Length Alternation. J. Am. Chem. Soc. 1994, 116, 2619-2620.
(115) Isborn, C. M.; Leclercq, A.; Vila, F. D.; Dalton, L. R.; Bredas, J. L.; Eichinger, B. E.; Robinson, B. H. Comparison of Static First Hyperpolarizabilities Calculated with Various Quantum Mechanical Methods. J. Phys. Chem. A 2007, 111(7), 1319-1327.
(116) Dalton, L. R.; Benight, S. J.; Johnson, L. E.; Knorr, Jr., D. B.; Kosilkin, I.; Eichinger, B. E.; Robinson, B. H.; Jen, A.; Overney, R. Systematic Nano-Engineering of Soft Matter Organic Electro-Optic Materials. Chem. Mater. 2011, 23, 430-445.
(117) Suponitsky, K. Y.; Liao, Y.; Masunov, A. E. Electronic Hyperpolarizabilities for Donor-Acceptor Molecules with Long Conjugated Bridges: Calculations Versus Experiment. J. Phys. Chem. A 2009, 113, 10994-11001.
(118) Johnson, L. E.; Dalton, L. R.; Robinson, B. H. Optimizing Calculations of Electronic Excitations and Relative Hyperpolarizabilities of Electrooptic Chromophores. Acc. Chem. Res. 2014, 47(11), 3258-3265.

(119) Korzdorfer, T.; Bredas, J. L. Organic Electronic Materials: Recent Advances in the DFT Description of the Ground and Excited States Using Tuned Range-Separated Hybrid Functionals. Acc. Chem. Res. 2014, 47(11), 3284-3291.
(120) Garrett, K.; Vasuez, X. A. S.; Egri, S. B.; Wilmer, J.; Johnson, L. E.; Robinson, B. H.; Isborn, C. M. Optimum Exchange for Calculation of Excitation Energies and Hyperpolarizabilities of Organic Electro-Optic Chromophores. J. Chem. Theory and Comput. 2014, 38l21-3831.
(121) Sullivan, P. A.; Dalton, L. R. The Material Genome for Organic Electro-Optics and Silicon/Plasmonic-Organic Hybrid Technology. New Horizons in Nanoscience and Engineering. Andrews, D. L.; Grote, J. G., eds. 2015, Chap. 6, 233-264.
(122) Takimoto, Y.; Isborn, C. M.; Eichinger, B. E.; Rehr, J. J.; Robinson, B. H. Frequency and Solvent Dependence of Nonlinear Optical Properties of Molecules. J. Phys. Chem. C 2008, 112, 8016-8021.
(123) Liang, W.; Li, X.; Dalton, L. R.; Robinson, B. H.; Eichinger, B. E. Solvents Leve Dipole Moments. J. Phys. Chem. B 2011, 115(43), 12566-12570.
(124) Bale, D. H.; Eichinger, B. E.; Liang, W.; Li, X.; Dalton, L. R.; Robinson, B. H.; Reid, P. J. Dielectric Dependence of the First Molecular Hyperpolarizability for Electro-Optic Chromophores. J. Phys. Chem. B 2011, 115(13), 3505-3513.
(125) Davidson, E. R.; Eichinger, B. E.; Robinson, B. H. Hyperpolarizability: Calibration of Theoretical Methods for Chloroform, Water, Acetonitrile, and p-Nitroaniline. Opt. Mater. 2006, 29(4), 360-364.
(126) Kocherzhenko, A. A.; Vacquez, X. A.; Milanese, J. M.; Isborn, C. M. Absorption Spectra for Disordered Aggregates of Chromophores Using the Exciton Model. J. Chem. Theory Comput. 2017, 13(8), 3787-3801.
(127) Kocherzhenko, A. A.; Sapana, S. V.; Vacquez, X. S.; Maat, J.; Wilmer, J.; Tillack A. F.; Johnson, L. E.; Isborn, C. M. Unraveling Excitonic Effects for the First Hyperpolarizabilities of Chromophore Aggregates. J. Phys. Chem. C 2019, 123(22), 13818-13836.
(128) Davies, J. A.; Elanogovan, A.; Sullivan, P. A.; Olbricht, B. C.; Bale, D. H.; Ewy, T. R.; Isborn, C. M.; Eichinger, B. E.; Robinson, B. H.; Reid, P. J.; Li, X.; Dalton, L. R. Rational Enhancement of Second-Order Nonlinearity: Bis-(4-methoxyphenyl)hetero-aryl-amino Donor-Based Chromophores: Design, Synthesis, and Electrooptic Activity. J. Am. Chem. Soc. 2008, 130, 10655-10575.
(129) Jin, W.; Johnson, P. V.; Elder, D. L.; Manner, K. T.; Garrett, K. E.; Kaminsky, W.; Xu, R.; Robinson, B. H.; Dalton, L. R. Structure-Function Relationship Exploration for Enhanced Thermal Stability and Electro-Optic Activity in Monolithic Organic NLO Chromophores. Mater. Chem. 2016, 4, 3119-3124.
(130) Elder, D. L.; Haffner, C.; Heni, W.; Fedoryshyn, Y.; Garrett, K. E.; Johnson, L. E.; Campbell, R. A.; Avila, J. D.; Robinson, B. H.; Leuthold, J.; Dalton, L. R. Effect of Rigid Bridge-Protection Units, Quadrupolar Interactions and Blending in Organic Electro-Optic Chromophores. Chem. Mater. 2017, 29, 6457-6371.
(131) Elder, D. L.; Johnson, L. E.; Tillack, A. F.; Robinson, B. H.; Haffner, C.; Heni, W.; Hoessbacher, C.; Fedoryshyn, Y.; Salamin, Y.; Baeuerle, B.; Josten, A.; Ayata, M.; Koch, U.; Leuthold, J.; Dalton, L. R. Multi-Scale Theory-Assisted Nano-Engineering of Plasmonic-Organic Hybrid Electro-Optic Device Performance. Proc. SPIE 2018, 10529, 10529OK.
(132) Johnson, L. E.; Elder, D. L.; Kocherzhenko, A. A.; Tillack, A. F.; Isborn, C. M.; Dalton, L. R.; Robinson, B. H. Poling-Induced Birefringence in OEO Materials Under Nanoscale Confinement. Proc. SPIE 2018, 10738, 107381A.
(133) Robinson, B. H.; Johnson, L. E.; Elder, D. L.; Kocherzhenko, A. A.; Isborn, C. M.; Haffner, C.; Heni, W.; Hoessbacher, C.; Fedoryshyn, Y.; Salamin, Y.; Baeuerle, B.; Josten, A.; Ayata, M.; Koch, U.; Leuthold, J.; Dalton, L. R. Optimization of Plasmonic-Organic Hybrid Electro-Optics. J. Lightw. Technol. 2018, 36(21), 5036-5047.
(134) Johnson, L. E.; Xu, H.; de Coene, Y.; Elder, D. L.; Clays, K.; Dalton, L. R.; Robinson, B. H. Next Generation Materials for Hybrid Electro-Optic Systems. Proc. SPIE 2019, 11089, 11089OK.
(135) Xu, H.; Liu, F.; Elder, D. L.; Johnson, L. E.; de Coene, Y.; Clays, K.; Robinson, B. H.; Dalton, L. R. Ultrahigh Electro-Optic Coefficients, High Index of Refraction, and Long-Term Stability from Diels-Alder Cross-Linkable Binary Molecular Glasses. Chem. Mater. 2020, 32, 1408-1421.
(136) Johnson, L. E.; Xu, H.; Hammond, S. R.; Elder, D. L.; Benight, S. J.; de Coene, Y.; Hesse-Withbroe, J.; Clays, K.; Dalton, L. R.; Robinson, B. H. Advances in High-Performance Hybrid Electro-Optics. Proc. SPIE 2020, 11471, 11471OB.
(137) Xu, H.; Johnson, L. E.; de Coene, Y.; Elder, D. L.; Hammond, S. R.; Clays, K.; Dalton, L. R.; Robinson, B. H. Bis (4-Dialkylaminopheny) Heteroarylamino Donor Chromophores Exhibiting Exceptional Hyperpolarizabilities. J. Mater. Chem. C 2021, 9(8), 2721-2728.

(138) Dalton, L. R.; Sullivan, P. A.; Bale, D. H. Electric Field Poled Organic Electro-Optic Materials: State of the Art and Future Prospects. Chem. Rev. 2010, 110, 25-55.
(139) Sullivan, P. A.; Dalton, L. R. Theory-Inspired Development of Organic Electro-Optic Materials. Acc. Chem. Res. 2010, 43(1), 10-18.
(140) Kang, H.; Facchetti, A.; Jiang, H.; Cariati, E.; Righetto, S.; Ugo, R.; Zuccaccia, C.; Macchioni, A.; Stern, C. L.; Liu, Z.; Ho, S. T.; Brown, E. C.; Ratner, M. A.; Marks, T. J. Ultralarge Hyperpolarizability Twisted π-Electron System Electro-Optic Chromophores: Synthesis, Solid-State and Solution-Phase Characteristics, Electronic Structures, Linear and Nonlinear Optical Properties, and Computational Studies. J. Am. Chem. Soc. 2007, 129, 3267-3286.
(141) Brown E. C.; Marks, T. J.; Ratner, M. A. Nonlinear Response Properties of Ultralarge Hyperpolarizability Twisted p-System Donor-Acceptor Chromophores Dramatic Environmental Effects on Response. J. Phys. Chem. B 2008, 112, 44-50.
(142) Wang, Y.; Frattarelli, D. L.; Facchetti, A.; Cariati, E.; Righetto, S.; Ugo, R.; Zuccaccia, C.; Macchioni, A.; Stern C. L.; Ratner, M. A.; Marks, T. J. Twisted π-Electron System Electro-Optic Chromophores: Structural and Electronic Consequences of Relaxing Twist-Inducing Non-Bonded Repulsions. J. Phys. Chem. C 2008, 112, 3005-3015.
(143) Isborn, C. S.; Robinson, B. H. Ab Initio Diradical/Zwiterionic Polarizabilities and Hyperpolarizabilities in Twisted Diradicals. J. Phys. Chem. A 2006, 110, 7189-7196.
(144) Kim, W. K.; Hyden, L. M. Fully Atomistic Modeling of a Electric Field Poled Guest-Host Nonlinear Optical Polymer. J. Chem. Phys. 1999, 111, 5212-5222.
(145) Leahy-Hoppa, M. R.; Cunningham, P. D.; French, J. A.; Hayden, L. M. Atomistic Molecular Modeling of the Effect of Chromophore Concentration on the Electro-Optic Coefficient in Nonlinear Optical Polymers. J. Phys. Chem. A 2006, 110, 5792-5797.
(146) Makowska-Janusik, M.; Reis, H.; Papadopoulos, M. G.; Economou, I. G.; Zacharopoulos, N. Molecular Dynamics Simulations of Electric Field Poled Nonlinear Optical Chromophores Incorporated in a Polymer Matrix. J. Phys. Chem. B 2004, 108, 588-596.
(147) Dalton, L. R.; Harper, A. W.; Robinson, B. H. The Role of London Forces in Defining Noncentrosymmetric Order in High Dipole Moment-High Hyperpolarizability Chromophores in Electrically Poled Polymeric Thin Films. Proc. Natl. Acad. Sci. USA 1997, 94(10), 4842-4547.
(148) Robinson, B. H.; Dalton, L. R. Monte Carlo Statistical Mechanical Simulations of the Competition of Intermolecular Electrostatic and Poling Field Interactions in Defining Macroscopic Electro-Optic Activity for Organic Chromophore/Polymer Materials. J. Phys. Chem. A 2000, 104(20), 4785-4795.
(149) Pereverzev, Y. V.; Prezhdo, O. V.; Dalton, L. R. Mean Field Theory of Acentric Order of Dipolar Chromophores in Polymeric Electro-Optic Materials. Chromophores with Displaced Dipoles. Chem. Phys. Lett. 2011, 340, 328-335.
(150) Pereverzev, Y. V.; Prezhdo, O. V.; Dalton, L. R. Sample Shape Influence on the Antiferroelectric Phase Transitions in Dipolar Systems Subject to an External Field. Phys. Rev. B: Condens. Mater. 2002, 65, 052101-4.
(151) Pereverzev, Y. V.; Prezhdo, O. V.; Dalton, L. R. A Model of Phase Transitions in the System of Electro-Optic Dipolar Chromophores Subject to an Electric Field. J. Chem. Phys. 2002, 117, 335-3360.
(152) Dalton, L. R.; Robinson, B. H.; Nielsen, R. D.; Jen, A. K.-Y.; Steier, W. H. Organic Electro-Optic: From Molecules to Devices. Proc. SPIE 2002, 4798, 1-10.
(153) Dalton, L. R.; Robinson, B. H.; Jen, A. K.-Y.; Steier, W. H.; Nielsen, R. D. Systematic Development of High Bandwidth, Low Drive Voltage Organic Electro-Optic Devices and Their Applications. Opt. Mater. 2003, 21, 19-28.
(154) Pereverzev, Y. V.; Prezhdo, O. V.; Dalton, L. R. Structural Origin of the Enhanced Electro-Optic Response of Dendrimeric Systems. Chem. Phys. Lett. 2003, 373, 207-212.
(155) Pereverzev, Y. V.; Prezhdo, O. V.; Dalton, L. R. Macroscopic Order and Electro-Optic Response of Dipolar Chromophore-Polymer Materials. Chem. Phys. Chem. 2004, 5, 1821-1830.
(156) Nielsen, R. D.; Rommel, H. L.; Robinson, B. H. Simulation of the Loading Parameter in Organic Nonlinear Optical Materials. J. Phys. Chem. B 2004, 25, 8659-8667.
(157) Rommel, H. L.; Robinson, B. H. Orientation of Electro-Optic Chromophores under Poling Conditions: A Spheroidal Model. J. Phys. Chem. C 2007, 111(50), 18765-18777.
(158) Sullivan, P. A.; Rommel, H. L.; Takimoto, Y.; Hammond, S. R.; Bale, D. H.; Olbricht, B. C.; Liao, Y.; Rehr, J.; Eichinger, B. E.; Jen, A. K.-Y.; Reid, P. J.; Dalton, L. R.; Robinson, B. H. Modeling the Optical

Behavior of Complex Organic Media: From Molecules to Materials. J. Phys. Chem. B 2009, 113(47), 15581-15588.
(159) Benight, S. J.; Johnson, L. E.; Barnes, R.; Olbricht, B. C.; Bale, D. H.; Reid, P. J.; Eichinger, B. E.; Dalton, L. R.; Sullivan, P. A.; Robinson, B. H. Reduced Dimensionality in Organic Electro-Optic Materials: Theory and Defined Order. J. Phys. Chem. B 2010, 114(37), 11949-11956.
(160) Benight, S. J.; Knorr, Jr., D. B.; Johnson, L. E.; Sullivan, P. A.; Lao, D.; Sun, J.; Kocherlakota, L.S.; Elangovan, A.; Robinson, B. H.; Overney, R. M.; Dalton, L. R. Nano-Engineering Lattice Dimensionality for a Soft Matter Organic Functional Material. Adv. Mater. 2012, 24(24), 3263-3268.
(161) Tillack, A. F.; Johnson, L. E.; Rawal, M.; Dalton, L. R.; Robinson, B. H. Modeling Chromophore Order: A Guide for Improving EO Performance. MRS Online Proceedings Library (OPL)-Cambridge University Press 2014, 1698, mrss14-1698-jj08-05.
(162) Elder, D. L.; Benight, S. J.; Song, J.; Robinson, B. H.; Dalton, L. R. Matrix-Assisted Poling of Monolithic Bridge-Disubstituted Organic NLO Chromophores. Chem. Mater. 2014, 26(2), 872-874.
(163) Robinson, B. H.; Johnson, L. E.; Eichinger, B. E. Relation of System Dimensionality and Order Parameters. J. Phys. Chem. B 2015, 119(7), 3205-3512.
(164) Johnson, L. E.; Benight, S. J.; Barnes, R.; Robinson, B. H. Dielectric and Phase Behavior of Dipolar Spheroids. J. Phys. Chem. B 2015, 119(16), 5240-5250.
(165) Tillack, A. F.; Johnson, L. E.; Eichinger, B. E.; Robinson, B. H. Systematic Generation of Anisotropic Coarse-Grained Lennard-Jones Potentials and Their Application to Ordered Soft Matter. J. Chem. Theory Comput. 2016, 12(9), 4362-4374.
(166) Tillack, A. F.; Robinson, B. H. Toward Optimal EO Response form ONLO Chromophores: A Statistical Mechanics Study of Optimizing Shape. J. Opt. Soc. Amer. B 2016, 33(12), E121-E129.
(167) Tillack, A. F.; Robinson, B. H. Simple Model for the Benzene Hexafluorobenzene Interaction. J. Phys. Chem. B 2017, 121(25), 6184-6188.
(168) Tillack, A. F.; Robinson, B. H. Shape Matters: The Case for Ellipsoids and Ellipsoidal Water. J. Phys.: Conf. Ser. 2017, 921(1), 012015.
(169) Halter, M.; Liao, Y.; Plocinik, R. M.; Coffey, D. C.; Bhattacharjee, S.; Mazur, U.; Simpson, G. J.; Robinson, B. H.; Keller, S. L. Molecular Self-Assembly of Mixed High-Beta Zwitterionic and Neutral Ground-State NLO Chromophores. Chem. Mater. 2008, 20(5), 1778-1787.
(170) Liao, Y.; Firestone, K. A.; Bhattacharjee, S.; Luo, J.; Haller, M. A.; Hau, S.; Anderson, C. A.; Lao, D.; Eichinger, B. E.; Robinson, B. H.; Reid, P. J.; Jen, A. K.-Y.; Dalton, L. R. Linear and Nonlinear Optical Properties of a Macrocyclic Trichromophore Bundle with Parallel-Aligned Dipole Moments. J. Phys. Chem. B 2006, 18, 1062-1067.
(171) Liao, Y.; Bhattacharjee, S.; Firestone, K. A.; Eichinger, B. E.; Raranji, R.; Anderson, C. A.; Robinson, B. H.; Reid, P. J.; Dalton, L. R. Antiparallel-Aligned Neutral-Ground State and Zwitterionic Chromophores as a Nonlinear Optical Material. J. Am. Chem. Soc. 2006, 128(21), 6847-6853.
(172) Wang, C.; Zhang, M.; Stern, B.; Lipson, M.; Loncar, M. Nanophotonic Lithium Niobate Electro-Optic Modulators. Optics Express 2018, 26(2), 1547-1555.
(173) Weigel, P. O.; Zhao, J.; Fang, K.; Al-Rubaye, H.; Trotter, D.; Hood, D.; Mudrich, J.; Dallo, C.; Pomerene, A. T.; Starbuck, A. L.; DeRose, C. T.; Lentine, A. L.; Rebeiz, G.; Mookherjea, S. Bonded Thin Film Lithium Niobate Modulator on a Silicon Photonic Platform Exceeding 100 GHz 3-dB Electrical Modulation Bandwidth. Optics Express 2018, 26(18), 23728-23739.
(174) He, M.; Xu, M.; Ren, Y.; Jian, J.; Ruan, Z.; Xu, Y.; Gao, S.; Sun, S.; Wen, X.; Zhou, L.; Liu, L.; Guo, C.; Chen, H.; Yu, S.; Liu, L.; Cai, X. High-Performance Hybrid Silicon and Lithium Niobate Mach-Zehnder Modulators for 100 $Gbits^{-1}$ and Beyond. Nat. Photon. 2019, 13, 359-364.
(175) Ahmed, A. N. R.; Nelan, S.; Shi, S.; Yao, P.; Mercante, A.; Prather, D. W. Subvolt Electro-Optic Modulator on Thin-Film Lithium Niobate and Silicon Nitride Hybrid Platform. Opt. Lett. 2020, 45(5), 1112-1115.
(176) Boynton, N.; Cai, H.; Gehl, M.; Arterburn, S.; Dallo, C.; Pomerene, A.; Starbuck, A.; Hood, D.; Trotter, D. C.; Friedmann, T.; DeRose, C. T.; Lentine, A. A Heterogeneously Integrated Silcion Photonic/Lithium Niobate Traveling Wave Electro-Optic Modulator. Optics Express 2020, 28(2), 1868-1884.
(177) Ma, H.; Chen, B.; Dalton, L. R.; Jen, A. K.-Y. Novel Perfluorocyclobutane-Containing Thermoset Polymers and Dendrimers in Electro-Optics. Polym. Mat. Sci. Eng. 2000, 83, 165-166.
(178) Zhang, C.; Wang, C.; Yang, J.; Dalton, L. R.; Sun, G.; Zhang, H.; Steier, W. H. Electric-Poling and Relaxation of Thermoset Polyurethane Second-Order Nonlinear Optical Materials: The Role of Cross-Linking and Monomer Rigidity. Macromolecules. 2001, 32(2), 235-243.

(179) Wang, C.; Zhang, C.; Lee, M. S.; Dalton, L. R.; Zhang, H.; Steier, W. H. Urethane-Urea Copolymers Containing Siloxane Linkages: Enhanced Temporal Stability and Low Optical Loss for Second-Order Nonlinear Optical Applications. Macromolecules. 2001, 34, 2359-2363.
(180) Dalton, L. R. Nonlinear Optical Polymeric Materials: From Chromophore Design to Commercial Applications. Advances in Polymer Science 2002, 158, 1-86.
(181) Dalton, L. R. Rational Design of Organic Electro-Optic Materials. J. Phys.: Condens. Matter 2003, 15, R897-R934.
(182) Zhang, C.; Zhang, H.; Oh, M.-C.; Dalton, L. R.; Steier, W. H. What the Ultimate Polymeric Electro-Optic Materials Will Be: Guest-Host, Crosslinked, or Side Chain. Proc. SPIE 2003, 4991, 537-551.
(183) Dalton, L. R. Organic Electro-Optic Materials. Pure and Applied Chemistry 2004, 76(7-8), 1421-1433.
(184) Haller, M.; Luo, J.; Li, H.; Kim, T.-D.; Liao, Y.; Robinson, B. H.; Dalton, L. R.; Jen, A. K.-Y. A Novel Lattice-Hardening Process to Achieve Highly Efficient and Thermally Stable Nonlinear Optical Polymers. Macromolecules 2004, 37(3) 688-690.
(185) Kim, T.-D.; Kang, J.-W.; Luo, J.; Jang, S.-H.; Ka, J.-W.; Tucker, N.; Benedict, J. B.; Dalton, L. R.; Gray, T.; Overney, R. M.; Park, D. H.; Herman, W. N.; Jen, A.-K. Ultralarge and Thermally Stable Electro-Optic Activities from Supramolecular Self-Assembled Molecular Glasses. J. Am. Chem. Soc. 2007, 129(3), 488-489.
(186) Sullivan, P. A.; Olbricht, B. C.; Akelaitis, A. J. P.; Mistry, A. A.; Liao, Y.; Dalton, L. R. Tri-component Diels-Alder Polymerized Dendrimer Glass Exhibiting Large, Thermally Stable, Electro-Optic Activity. J. Mater. Chem. 2007, 17, 2899-2903.
(187) Shi, Z.; Hau, S.; Luo, J.; Kim, T.-D.; Tucker, N. M.; Ka, J.-W.; Sun, H.; Pyayt, A.; Dalton, L. R.; Chen, A.; Jen, A. K.-Y. Highly Efficient Diels-Alder Crosslinkable Electro-Optic Dendrimers for Electric-Field Sensors. Adv. Funct. Mater. 2007, 17, 2557-2563.
(188) Shi, Z.; Luo, J.; Huang, S.; Cheng, Y.-J.; Kim, T.-D.; Polishak, B. M.; Zhou, X.-H.; Tian, Y.; Jang, S.-H.; Knorr Jr., D. B.; Overney, R. M.; Younkin, T. R.; Jen, A. K.-Y. Controlled Diels-Alder Reactions Used to Incorporate Highly Efficient Polyenic Chromophores into Maleimide-Containing Side-Chair Polymers for Electro-Optics. Macromolecules 2009, 42(7), 2438-2445.
(189) Shi, Z.; Liang, W.; Luo, J.; Huang, S.; Polishak, B. M.; Li, X.; Younkin, T. R.; Block, B. A.; Jen, A. K.-Y. 2010, Chem. Mater. 22(19), 5601-5608.
(190) Shi, Z.; Cui, Y. Z.; Li, Z.; Luo, J.; Jen, A. K.-Y. Dipolar Chromophore Facilitated Huisgen Cross-Linking Reactions for Highly Efficient and Thermally Stable Electrooptic Polymers. ACS Macro Lett. 2012, 37(15), 793-796.
(191) Shi, Z.; Luo, J.; Huang, S.; Polishak, B. M.; Zhou, X. H.; Liff, S.; Younkin, T. R. Achieving Excellent Electro-Optic Activity and Thermal Stability in Poled Polymers Through an Expeditious Crosslinking Process. J. Mater. Chem. 2012, 22(3), 951-959.
(192) Jin, W.; Johnston, P. V.; Elder, D. L.; Manner, K. T.; Garrett, K. E.; Kaminsky, W.; Xu, R.; Robinson, B. H.; Dalton, L. R. Structure-Function Relationships Exploration for Enhanced Thermal Stability and Electro-Optic Activity in Monolithic Organic NLO Chromophores. J. Mater. Chem. C 2016, 4(15), 3119-3124.
(193) Wu, J.; Wu, B.; Wang, W.; Chiang, K. S.; Jen, A. K.-Y.; Luo, J. Ultra-Efficient and Stable Electro-Optic Dendrimers Containing Supramolecular Homodimers of Semifluorinated Dipolar Aromatics. Materials Chemistry Frontiers 2018, 2(5), 901-909.
(194) Xu, H.; Liu, F.; Elder, D. L.; Johnson, L. E.; de Goene, Y.; Clays, K.; Robinson, B. H.; Dalton, L. R. Ultrahigh Electro-Optic Coefficients, High Index of Refraction, and Long-Term Stability from Diels-Alder Crosslinkable Binary Molecular Glasses. Chem. Mater. 2020, 32(4), 1408-1421.
(195) Liu, J.; Si, P.; Liu, X.; Zhen, Z. Copper-Catalyzed Huisgen Cycloaddition Reactions Used to Incorporate NLO Chromophores into High Tg Side-Chain Polymers for Electro-Optics. Opt. Mater. 2015, 47, 256-262.
(196) Spring, A. M.; Qiu, F.; Hong, J.; Bannaron, A.; Kashino, T.; Kikucki, T.; Ozawa, M.; Nawata, H.; Odoi, K.; Yokoyama, S. Crosslinked Poly(norbornene-dicarboximide)s as Electro-Optic Chromophore Hosts. Eur. Polym. J. 2017, 97, 263-271.
(197) Miura, H.; Qiu, F.; Spring, A. M.; Kashino, T.; Kikuchi, T.; Ozawa, M.; Nawata, H.; Odoi, K.; Yokoyama, S. High Thermal Stability 40 GHz Electro-Optic Polymer Modulators. Optics Express 2017, 25(23), 28643-28649.

(198) Kieninger, C.; Kutuvantavida, Y.; Miura, H.; Kemal, J. N.; Zwickel, H.; Qiu, F.; Lauermann, M.; Freude, W.; Randel, S.; Yokoyama, S.; Koos, C. Demonstration of Long-Term Thermally Stable Silicon-Organic Hybrid Modulators at 85°C. Optics Express 2018, 26(21), 27955-27964.
(199) Lu, G.-W.; Hong, J.; Qiu, F.; Spring, A. M.; Kashino, T.; Oshima, J.; Ozawa, M.-A.; Nawata, H.; Yokoyama, S. High-Temperature-Resistant Silicon-Polymer Hybrid Modulator Operating at up to 200 Gbit s-1 for Energy Efficient Datacentres and Harsh-Environment Applications. Nat. Commun. 2020, 11, 4224.
(200) Benight, S. J.; Hammond, S. R.; Johnson, L. W.; Elder, D. L. Processing of Organic Electro-Optic Materials for Commercial Applications. Proc. SPIE 2020, 11467, 1144671H.
(201) Dinu, R.; Jin, D.; Yu, G.; Chen, B.; Huang, D.; Chen, H.; Barklund, A.; Miller, E.; Wei, C.; Vemagiri, J. Environmental Stress Testing of Electro-Optic Polymer Modulators. J. Lightw. Technol. 2009, 27(1), 1537-1532.
(202) Rezzonico, D.; Jazbinsek, M.; Gunter, P.; Bosshard, C.; Bale, D. H.; Liao, Y.; Dalton, L. R.; Reid, P. J. Photostability Studies of p-Conjugated Chromophores with Resonant and Nonresonant Light Excitation for Long-Life Polymeric Telecommunication Devices. J. Opt. Soc. Amer. B 2007, 24, 2199-2207.
(203) Tominari, Y.; Yamada, T.; Kaji, T.; Yamada, C.; Otomo, A. Photostability of Organic Electro-Optic Polymer Under Practical High Intensity Continuous-Wave 1500-nm Laser Irradiation. Jap. J. Appl. Phys. 2021, 60, 101002.
(204) https://money.cnn.com/news/newsfeeds/articles/prnewswire/CL01687.htm. 11/28/21.
(205) Zhang, C.; Taylor, E. W. Radiation Resistance of a Gamma-Ray Irradiated Nonlinear Optic Chromophore. J. of Nanophotonics 2009, 3(1), 031860.
(206) Kuzyk, M. G.; Dirk, C. W. Characterization Techniques and Tabulations for Organic Nonlinear Optical Materials. 1998, Marcel Dekker, New York.
(207) Park, D. H.; Lee, C. H.; Herman, W. N. Analysis of Multiple Reflection Effects in Reflective Measurements of Electro-Optic Coefficients of Poled Polymers in Multilayer Structures. Opt. Exp. 2006, 14(19), 8856-8884.
(208) Ullah, F.; Deng, N.; Qiu, F. Recent Progress in Electro-Optic Polymer for Ultra-Fast Communication. PhotoniX 2021, 2, 13.
(209) Minkenberg, C.; Krishnaswamy, R.; Zilkie, A.; Nelson D. Co-Packaged Datacenter Optics: Opportunities and Challenges. IET Optoelectronics. 2021, 15(2), 77-91.
(210) Nagarajan, R.; Lyubomirsky, I.; Agazzi, O. Low Power DSP-Based Transceivers for Data Center Optical Fiber Communications. J. Lightw. Technol. 2021, 39(16), 5221-5231.
(211) Miller, D. A. B. Atttojoule Optoelectronics for Low-Energy Information Processing and Communications. J. Lightw. Technol. 2017, 35(3), 346-396.
(212) Eppenberger, M.; Bitachon, B. I.; Messner, A.; Heni, W.; Habegger, P.; Destraz, M.; De Leo, E.; Meier, N.; Del Medico, N.; Hoessbacher, C.; Baeuerle, B.; Leuthold, J. Plasmonic Racetrack Modulator Transmitting 220 Gbit/s OOK and 408 Gibt/s 8PAM. 2021 European Conference on Optical Communication (ECOC), 2021, pp. 1-4 (doi: 10.1109/ECOC52684.2021.9605911).
(213) Hu, Q.; Borkowski, R.; Lefevre, Y.; Buchali, F.; Bonk, R.; Schuh, K.; De Leo, E.; Habegger, P.; Destraz, M.; Del Medico, N.; Duran, H.; Tedaldi, V.; Funck, C.; Fedoryshyn, Y.; Leuthold, J.; Heni, W.; Baeuerle, B.; Hoessbacher, C. Plasmonic-MZM-Based Short-Reach Transmission up to 10 km Supporting > 304 GBd Polybinary or 432 Gbit/s PAM-8 Signaling. 2021 European Conference on Optical Communication (ECOC), 2021, pp. 1-4 (doi: 10.1109/ECOC52684.2021.9606060).